sPH-TRG-2023-01

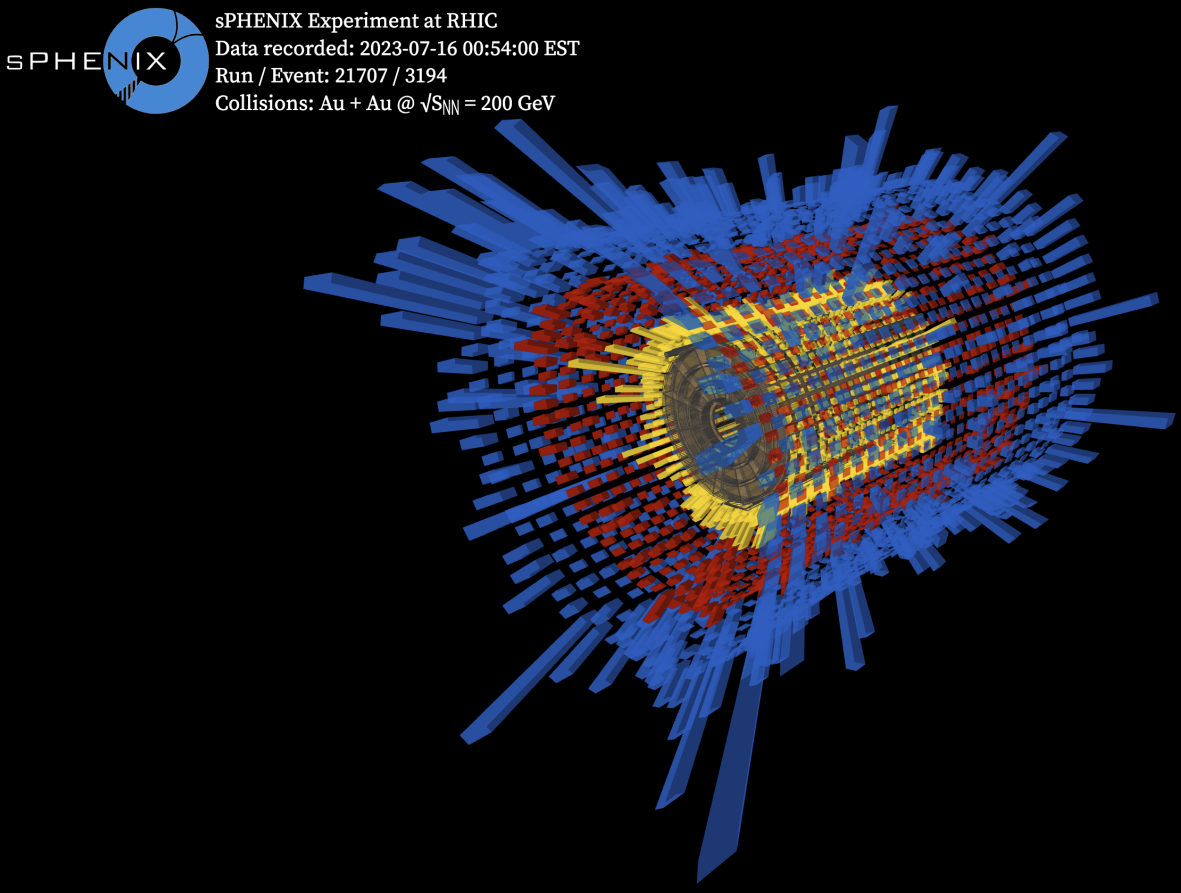

Central Au+Au data event recorded in the sPHENIX calorimeter system.

sPHENIX Beam Use Proposal

August 25, 2023

Executive Summary

sPHENIX is the first new collider detector at RHIC in over twenty years, with the goal of bringing new measurement capabilities for the exploration of the Quark-Gluon Plasma (QGP) not previously available in this energy range. The experiment is a specific priority of the DOE/NSF NSAC 2015 Nuclear Physics Long Range Plan (LRP) and has been widely endorsed in the community planning process for the 2023 LRP in progress. The significance of the expected results from sPHENIX, complementing those coming from the LHC, is additionally highlighted in the "Working Group 5: Heavy-Ion" input to the European Strategy for Particle Physics. sPHENIX was designed to play a critical role in the completion of the RHIC science mission by enabling qualitatively new measurements of the microscopic nature of the QGP.

We stress that the sPHENIX science program relies on very high delivered luminosities to complete its science mission. The large luminosity, together with the high rate and large acceptance of the detector, precise tracking, and electromagnetic and hadronic calorimetry, will enable measurements of jet production and substructure, and open and hidden heavy flavor over an unprecedented kinematic range at RHIC.

Construction and installation of the full sPHENIX detector, including the DOE Major Item of Equipment (MIE) project as well as additional subdetectors funded as BNL capital projects (e.g., the micro-vertex detector, MVTX), realized as contributions from collaborating institutions (e.g., the intermediate silicon strip tracker, INTT, and the TPC Outer Tracker, TPOT), or via NSF funding (e.g., the event plane detector, sEPD), was completed in 2023.

The process of commissioning the sPHENIX experiment with Au+Au beams began on May 18, 2023, with the receipt of approval to operate by BHSO (the Brookhaven site office of DOE). After approximately eleven weeks, the run ended prematurely for the year on August 1, 2023 by the unexpected shutdown of the RHIC machine. While all detector sub-systems made major progress towards a full commissioning, sPHENIX will require a dedicated period in 2024 to finish the commissioning process for key sub-detectors and thus be ready for full-luminosity physics data-taking. The commissioning status is described in a standalone, accompanying document to this Beam Use Proposal, including a detailed list of remaining commissioning tasks.

This document responds to a charge (see Appendix A) from the BNL NPP Associate Laboratory Director (ALD) to detail the sPHENIX run plan during the years 2024 and 2025, where the final year of data-taking is dictated by BNL's reference schedule for the Election Ion Collider (EIC). The charge is to assume that the 2024 run will include an additional six cryo-weeks of Au+Au running to make up for the early termination of 2023 run, but without specific guidance as to how those six weeks are placed in the overall run plan.

Based on the RHIC experience in Year-1, on August 7, 2023, C-AD updated the projected luminosity production of the machine for Year-2 (2024) and Year-3 (2025) running, resulting in significantly reduced luminosities compared to those used as the basis for the sPHENIX project's scientific proposal and for previous Beam Use Proposals. As a result of the observed performance of the machine in 2023, the previous "minimum" luminosity targets in 2024 and 2025 (which were based on the best performance observed in 2015 and 2016) are now instead listed as the maximum achievable – i.e. the projection is that the RHIC performance in 2024 and 2025 will be, at best, equal to that in 2015 and 2016.

For example, the projected weekly Au+Au luminosity production with large crossing angle for Run-2025 has been reduced by a factor of six compared to projections for that year made earlier in 2023. However, due to the sPHENIX data-taking strategy, a re-optimization of the beam-beam crossing angle in IP8 under the new conditions may result in a smaller reduction factor, while still meeting the constraint on charge deposition in the TPC. For the projections here, we consider a $\theta = 1$ mrad crossing angle scheme which results in a reduction of only 2.4 in the statistics for most observables in the sPHENIX physics program. The Collaboration is also committed to exploring further running and data-taking configurations which may optimize this further and recover additional luminosity. However, even in this case, we note that the lower projected luminosities, if realized in actual 2024 and 2025 running, would have a negative impact on many of the envisioned flagship measurements of the sPHENIX program, including those based around b-jets, the family of Upsilon states, and photon–jet pairs.

In this Beam Use Proposal, the sPHENIX collaboration outlines a plan which, following the latest understanding of the RHIC performance, has the best opportunity to fulfill the science mission of sPHENIX and RHIC as envisioned in the Long Range Plan. At the same time, we strongly urge that BNL explore any and all opportunities for sPHENIX to accumulate additional integrated luminosity for all collision systems.

Table 1 provides an overview of the request for Year-2 (2024) and Year-3 (2025), in response to the parameters in the ALD charge. The proposal is described in full detail in Chapter 2.

In Year-2 (2024), sPHENIX will require dedicated time to complete its commissioning process in Au+Au and to adjust to the beam conditions and experimental needs of transversely polarized p+p running. The optimal sequencing of collision species in Run-24 may depend on updated C-AD guidance and the result of sPHENIX cosmic commissioning over the coming months, and should be decided at an appropriate time. For this proposal, we consider two example scenarios (A and B) corresponding to cases where the additional Au+Au running occurs at the beginning and end of the 2024 run, respectively, with different potential benefits for the two cases. For example, putting Au+Au at the beginning may lessen the dedicated commissioning time needed in p+p, while putting it at the end would allow for the possibility of recording Au+Au data in full physics mode before the critical 2025 Au+Au run. These scenarios are meant to give specific quantitative examples, and it is expected that more detailed information from C-AD, developing information about sPHENIX readiness, and the progress of the 2024 run itself will help decide on a particular scenario. This could potentially include alternative plans, such as switching to Au+Au running in the middle of the run to avoid the impact of the high temperatures in the summer, or to ask for those six cryo-weeks to be used for additional p+p running.

With the reduced luminosity projections from C-AD, sPHENIX expects that it will be necessary to

Table 1: Summary of the sPHENIX Beam Use Proposal for 2024 and 2025, as requested in the charge. The values separated by slashes correspond to different cryo-week scenarios (20/24/28 in 2024 and 24/28 in 2025). The 10%-*str* values correspond to the modest streaming readout upgrade of the tracking detectors. Full details are provided in Chapter 2.

Species	$\sqrt{s_{NN}}$ [GeV]	Physics Weeks	Min. Bias Rec. Lum. $\lvert z\rvert$ <10 cm	Calo. Trigger Lum. $\lvert z\rvert$ <10 cm
Run-2024, Scenario A, 6 cryo-weeks Au+Au + 20/24/28 cryo-weeks p+p				
Au+Au	200	n/a	n/a (Commissioning running)	
p+p	200	13/17/21	0.34/0.44/0.54 pb^{-1} [@ 5kHz] 2.3/3.1/3.9 pb^{-1} [10%-str]	23/31/39 pb^{-1}
Run-2024, Scenario B, 20/24/28 cryo-weeks p+p + 6 cryo-weeks Au+Au				
p+p	200	9/13/17	0.23/0.34/0.44 pb^{-1} [@ 5kHz] 1.5/2.3/3.1 pb^{-1} [10%-str]	15/23/31 pb^{-1}
Au+Au	200	3	0.4 nb^{-1} (3B events)	not needed
Run-2025, 24/28 cryo-weeks				
Au+Au	200	20.5/24.5	5.2/6.3 nb^{-1} (35B/43B events)	not needed

have every available cryo-week in 2024[1] dedicated to p+p running, in order to obtain sufficient statistics for *in situ* calibrations of the detector, for the Cold QCD physics program, and to provide the vacuum QCD reference for the Au+Au program. We highlight that a modest streaming readout upgrade of the tracking detectors [10%-*str*], which is now in development and requires no additional hardware, will greatly extend this physics program.

We stress the critical need for high-luminosity p+p reference data for the sPHENIX physics program. Because of this need, there is no request for p+Au running in 2024 within any of the three requested cryo-week scenarios. We urge BNL to identify possible opportunities for additional cryo-weeks in future years which might enable p+Au running and the exciting physics that it would provide (as described in Appendix B).

The Year-3 (2025) request is focused on the collection of as large a Au+Au data set as possible for measurements of jets and heavy flavor observables with unprecedented precision and accuracy.

This document is organized as follows. Chapter 1 provides a brief summary of the sPHENIX physics program and project. Chapter 2 details the Year-2 and Year-3 (2024-2025) Beam Use Proposal from sPHENIX including a break down in terms of cryo-weeks. Chapter 3 presents selected physics

[1] i.e. with the possible exception of those carried over from 2023 for Au+Au running.

projections from the envisioned sPHENIX science program using 2024 and 2025 data. Chapter 4 provides a summary.

A separate document accompanying this one, titled "Commissioning Status: August 2023" gives a detailed report on each detector subsystem and provides an overview of the remaining commissioning plan for sPHENIX before and during the start of the 2024 run.

Additional information which may be of interest is included in the appendices. Appendix A contains the BUP charge from the ALD. Appendix B documents the physics output from possible p+Au data-taking in sPHENIX, should the opportunity arise.

An additional three appendices are archival in nature, documenting key aspects of RHIC running and sPHENIX readout capabilities, but not necessarily updated with the latest specific information on, e.g., expected RHIC capabilities. Appendix C documents some inputs to the luminosity projections from C-AD related to the beam-beam crossing angle. Appendix D documents modest upgrades to sPHENIX for the streaming readout capability. Finally, Appendix E outlines an alternative plan for potential post-2025 running of high-luminosity p+p, Au+Au, and small collision systems (such as O+O and Ar+Ar).

Contents

Chapter 1

sPHENIX Overview

1.1 Science Mission

Over the last decades, experiments at RHIC and LHC have shown that collisions of heavy nuclei produce a hot and dense state of matter, called Quark-Gluon Plasma (QGP). These studies demonstrated that the QGP is unique among all forms of matter in terms of its viscosity η/s, opacity, and vorticity. The QGP is a key example of a class of strongly coupled systems found recently in a wide range of areas of physics, from string theory to condensed matter and ultra-cold atom systems.

While measurements have provided detailed knowledge of the QGP's macroscopic (long wavelength) properties, we do not yet understand how these properties arise from the fundamental interactions of its constituents, i.e., quarks and gluons governed by the laws of Quantum Chromodynamics (QCD). In the 2015 Hot QCD Whitepaper [1] and the US Nuclear Physics Long Range Plan (LRP) [2], one of two highest priority goals in the field of Hot QCD was to "Probe the inner workings of QGP by resolving its properties at shorter and shorter length scales. The complementarity of the two facilities [i.e., RHIC and LHC] is essential to this goal, as is a state-of-the-art jet detector at RHIC, called sPHENIX" [2]. sPHENIX features prominently in contributed white papers [3] and town hall summaries [4] as part of the ongoing Long-Range Planning process in 2023 and, for example, in community-organized workshops [5].

To elucidate the nature of the QGP, the sPHENIX physics program rests on measurements using hard probes that are sensitive to the QGP microscopic structure over a broad range of length or momentum scales. These measurements at the top RHIC energy of $\sqrt{s_{NN}} = 200$ GeV include in particular studies of jet production and substructure, quarkonium suppression and open heavy flavor production and correlations. The sPHENIX studies will complement those planned at LHC for Run 3 during high luminosity Pb+Pb operations and provide qualitative improvements over current measurements at RHIC for related observables. While the existing RHIC measurements have greatly contributed to our understanding of the QGP, the overall kinematic range for many inclusive jet and photon+jet observables is constrained to $p_T < 20$ GeV even for the highest statistics measurements and is therefore insufficient for a direct comparison to LHC studies. In contrast, the projected sPHENIX measurements reach sufficiently high p_T to provide a significant overlap with the low range of measurements at the LHC, allowing to study identical hard probes embedded into QGP with different initial conditions and expansion dynamics.

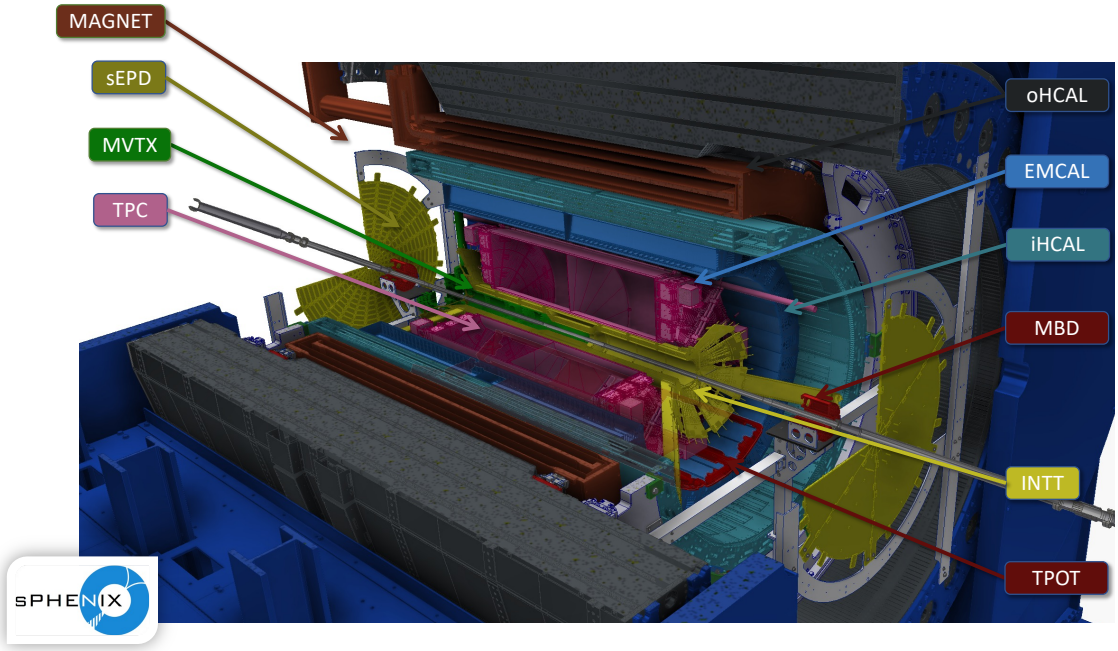

Figure 1.1: Engineering drawing (cutaway) of the sPHENIX detector. From the inside out the drawing shows the four tracking sub-systems (MVTX, INTT, TPC, and TPOT), the three calorimeter systems (EMCal, iHCal, and oHCal), the superconducting magnet, and two global detector sub-systems (MBD and sEPD). The ZDC and SMD are situated further away along the beam directions and are not shown. A detailed discussion of the sPHENIX detector subsystems can be found in the sPHENIX Technical Design Report [6].

In addition, the transversely polarized proton beams at RHIC will further enable key measurements of cold QCD including measurements of transverse single-spin asymmetries emerging from collinear twist-3 or parton transverse-momentum dependent (TMD) effects. If the opportunity for future p+Au collisions in RHIC should arise, they would enable key measurements of small-system collectivity in jet, hadron, and heavy flavor production.

sPHENIX was proposed by the PHENIX collaboration in their 2010 Decadal Plan as an upgrade (or replacement) of the PHENIX experiment at RHIC. The physics case and detector design were further developed in the years leading up to the 2015 Nuclear Physics LRP. A detailed design proposal was completed in 2015 [7], and in early 2016 the current sPHENIX collaboration was formed. As of 2023, sPHENIX has more than 360 members from 82 institutions in 14 countries. The project received DOE CD-0 approval in late 2016, CD-1/3A approval in 2018 and entered its construction phase after PD 2/3 approval in fall 2019. The process of commissioning the detector with beam began in May 2023 but did not fully conclude given the unexpected ending of the RHIC 2023 run. sPHENIX is thus planned to finish commissioning and take first physics data in 2024. The current expectation for 2025 as the final year of sPHENIX operations is dictated by BNL's reference schedule for the EIC project.

1.2 sPHENIX Design Highlights

The layout of the sPHENIX detector is shown in Figure 1.1. The experiment has been designed to enable high-statistics, high-resolution measurements for a broad range of observables related to jet production and modification, quarkonium production at high mass (or high p_T), and yields and correlations of heavy quark (charm and bottom) hadrons and heavy flavor tagged jets. This is achieved through several advances compared to the current instrumentation at RHIC:

- High data rates: the sPHENIX tracking and calorimetry provide hermetic coverage over full azimuth and pseudorapidity $|\eta| < 1$, with a readout rate of 15 kHz for all subdetectors. The detector also provides triggering capabilities in p+p, and for selected observables in Au+Au, as well as the option for streaming readout of the tracking detectors. In combination, statistical precision compared to the current status at RHIC will improve by 1-2 orders of magnitude for many observables.
- High resolution vertexing: the MAPS-based micro-vertex detector, MVTX, provides larger acceptance, faster readout, and higher resolution compared to previous RHIC detectors, enabling a state-of-the-art open heavy flavor program, including a large set of b-hadron measurements.
- Hadronic calorimetry: as a first at RHIC, sPHENIX features large acceptance hadronic calorimetry at mid-rapidity, enabling unbiased selection (and triggering in p+p) for jets, as well as improving the jet energy resolution and extending the range for high-p_T single hadron measurements through the rejection of mis-reconstructed tracks. In combination with the MVTX, this will allow the first application of b-jet tagging at RHIC.

1.3 sPHENIX Project

The sPHENIX detector is realized via several projects that are coordinated under a common project management structure. There are the elements of the original DOE Major Item of Equipment (MIE) — the outer hadronic calorimeter (oHCal), the central rapidity portion of electromagnetic calorimeter (EMCal) covering $|\eta| < 0.85$, the time projection chamber (TPC), and their associated readout electronics and services. The silicon strip tracker (INTT) is provided by RIKEN. Additional tungsten/scintillating fiber blocks extending the coverage of the EMCal to $|\eta| < 1.1$ have been provided by a consortium of collaborating institutions. The inner longitudinal section of the hadronic calorimeter (iHCal) and the silicon pixel vertex detector (MVTX) were successfully pursued as BNL capital projects. The sPHENIX event plane detector (sEPD) was funded by an National Science Foundation (NSF) Major Research Instrument (MRI) grant. A quartz Čerenkov minimum bias detector, originally built by Hiroshima University for the PHENIX experiment, was re-purposed for use in sPHENIX. There were also BNL funded projects to upgrade the infrastructure at IP8, to operate the 1.4 T BaBar superconducting solenoid, and to integrate and install the sPHENIX detector into the IP8 area.

The sPHENIX MIE received Critical Decision CD-1/3A approval in August 2018, followed by (after it moved from the CD process to the BNL-managed Project Decision (PD) process) PD-2/3 approval in September 2019, and has undergone regular Cost & Schedule reviews.

All detector subsystems were installed by Spring 2023 and the MIE was thus successfully completed. sPHENIX was given approval to operate on May 18th, 2023, with first beam collisions following nearly immediately to begin the sPHENIX commissioning run at RHIC. Further details on the status of each subsystem are provided in the commissioning document which accompanies this Beam Use Proposal.

The MIE scope consists of six detector projects and management of the MIE and related projects. The detector systems are:

- The compact (80 cm radius), ungated Time Projection Chamber (TPC), with GEM-based readout digitized via modified SAMPA ASICs, which were developed for the ALICE experiment
- The electromagnetic calorimeter, a tungsten-scintillating fiber SPACAL read out with solid state photomultiplier (SiPM's)
- The outer hadronic calorimeter, tilted steel plates with scintillating tiles interspersed in slots, also read out with SiPMs, which also doubles as the flux return of the 1.5 T superconducting solenoid
- Common electronics to read out both calorimeters consisting of shaper amplifiers on the detector which bring analog signals to 60 MHz waveform digitizers outside the solenoid
- Data acquisition designed to be capable of taking minimum bias Au+Au collisions at 15 kHz with greater than 90% livetime, and minimum bias triggers for Au+Au collisions, and jet and photon triggers for p+p and p+A operation
- The Minimum Bias Detector (MBD), which consists of the refurbished PHENIX Beam-Beam Counter (BBC), read out and triggered with new electronics based on the digitizers designed for the calorimeters

Non-MIE elements of the project include:

- The support structure of the electromagnetic calorimeter has been instrumented with scintillating tiles similar to the tiles used in the Outer HCal as part of the Inner HCal project, providing an additional ≈ 0.3 nuclear interaction lengths to catch the start of developing hadronic showers before they pass through the (uninstrumented) magnet.
- The section of the barrel EMCal with $|\eta| > 0.85$ was de-scoped before CD-1/3A, however it has been restored through collaboration with institutions in China and assembled normally together with the UIUC-produced blocks into EMCal sectors.
- The detector nearest the collision point is the MVTX, a silicon pixel detector closely based on the ALICE ITS inner barrel using Monolithic Active Pixel Sensors (MAPS). The MVTX is capable of 5 μm resolution for tracks with $p_T > 1$ GeV and enables the heavy-flavor tagged jet and open heavy-flavor programs.
- The INTT is a silicon strip detector surrounding the MVTX. This detector interpolates tracks between the extremely fine pitch of the MVTX and the coarser spatial resolution of the TPC. It is also the only tracking detector with single-beam-crossing timing resolution — the ability

to uniquely associate hits with a specific bunch crossing — and is therefore key to associating fully reconstructed tracks with the event that produced them.

- The sPHENIX Event Plane Detector (sEPD) consists of two wheels of scintillator tiles positioned at $2 < |\eta| < 4.9$. The sEPD, similar to the existing STAR EPD, provides significantly improved event plane (EP) resolution compared to the MBD with a large rapidity gap between the EP determination and the mid-rapidity measurement region. The sEPD is funded by a NSF MRI grant with Lehigh, UNC Greensboro, CU Boulder, Muhlenburg, and BNL as participating institutions.
- The TPC Outer Tracker (TPOT) is a Micromegas-based tracker consisting of eight modules situated between the bottom side of the TPC and the EMCal. The TPOT helps monitor space-charge distortions in the TPC by providing, for tracks in select fraction of the acceptance, a space point at a known location to improve track extrapolation accuracy from the MVTX and INTT into the TPC. TPOT is a collaborative effort between groups at CEA-Saclay, LANL, MIT and BNL.

A separate Infrastructure and Facility Upgrade project consisted of modifications to the 1008 facility needed to support the MIE and other detectors, most importantly support of the former BaBar solenoid into the RHIC cryogenic and power supply systems. All the support systems for the detector, such as the power distribution and safety systems, and the integration and installation of the detector are designed and managed as part of this project. While the planned sPHENIX beam pipe was lost in a transit accident in early 2022, a replacement beam pipe from STAR was successfully modified for use in the interaction region.

Chapter 2

Beam Use Proposal 2024–2025

In this Chapter we detail the sPHENIX Beam Use Proposal as requested in the Associate Laboratory Director Charge for the running period 2024–2025. We assume scenarios of 20, 24, or 28 weeks in 2024 (with an additional six weeks for Au+Au running), and 24 or 28 weeks in 2025. The complete charge is reproduced in Appendix A.

2.1 RHIC Luminosity Projections

For planning purposes, C-AD provides luminosity projections in a periodically updated document which utilizes knowledge gained from recent runs, most relevantly the Au+Au 2023 experience. The most recent version is always available at: `http://www.rhichome.bnl.gov/RHIC/Runs/RhicProjections.pdf` , and as of this writing is dated 7 August 2023.

From 2019 to mid-2022, the versions of this document featured a stable set of projections which were used for the preparation of the Beam Use Proposals in 2020, 2021 and 2022. On May 3, 2022, C-AD released updated guidance in which the p+p projections were moderately decreased (by a factor of approximately 0.2) compared to expectations, but p+Au and Au+Au projections were largely unchanged. This update was not included for the BUP 2022, which was submitted May 18, 2022. On August 7, 2023, the C-AD guidance was significantly updated given the experience of the 2023 run. The impact for p+p running is a decrease in the weekly luminosity production by a factor of 0.4, thus combining to a factor of approximately 2 considering this change together with the one from summer 2022. For the Au+Au running, the weekly delivered luminosity has fallen by a factor of six, due to a decrease in both delivered luminosity (factor of 2.3) and in the fraction of how the luminosity decreases under a finite beam-beam crossing angle (additional factor of 2.6). However, we believe that by optimizing the crossing angle and due to the particular minimum-bias data-taking strategy in sPHENIX, the reduction factor is approximately 2.4 for most observables, and that further optimization of the running and data-taking configurations may result in a larger recovered luminosity.

The quantitative projections in this Chapter are based on this recent guidance. However, given its very recent arrival, the physics projection plots in Chapter 3 are reproduced from the sPHENIX BUP 2022, along with a description of the quantitative impact of the lower luminosity.

Crossing angle θ	$L(\theta,$ all $z)/$ $L(\theta = 0,$ all $z)$	$L(\theta, \lvert z\rvert < 10$ cm$)/$ $L(\theta,$ all $z)$	σ_z in sPHENIX [cm]	Lumi/Week all z [μb^{-1}]	Lumi/Week ($\lvert z\rvert < 10$ cm) [μb^{-1}]
0 mrad	1.0	0.30	26	2210	660
1 mrad	0.30	0.52	14	660	340
2 mrad	0.15	0.79	8	330	260

Table 2.1: Summary of projected 2025 Au+Au luminosity production under different crossing angle scenarios. The luminosity/week is based on the average of the minimum and maximum projection. The vertex width σ_z, and thus the vertex factor $L(\theta, |z| < 10 \text{ cm})/L(\theta, \text{ all } z)$, is taken from direct measurements in sPHENIX in 2023 Au+Au running, as suggested by C-AD. All other values are taken directly from C-AD guidance. The right column, which is the luminosity per week within the narrow vertex, is the relevant quantity for sPHENIX physics.

We describe the quantitative translation of the C-AD projections into expected event rates at sPHENIX for 2024-2025 below. In the planning document, C-AD provides a minimum and maximum luminosity per week for each running period, under different crossing-angle scenarios. In previous projection documents, C-AD would directly provide the fraction of collisions within a given z-vertex range. However, these quantities are no longer available as direct input in the document and fraction of the luminosity within $|z| < 10$ cm, i.e. the usable collisions for the sPHENIX tracking system, must be calculated in other ways. For p+p running, this so-called narrow-z-vertex fraction was given to sPHENIX via private communication by Wolfram Fischer. For Au+Au running, the C-AD recommendation was to use the reconstructed z-vertex width observed by sPHENIX in 2023 Au+Au running (see commissioning document). Table 2.1 compares the relevant quantities for Au+Au luminosity production usable by sPHENIX under different crossing angles.

For calculating the integrated luminosity, we assume a progressive ramp-up curve over a three-week period described below in Chapter 2.3. This is then followed by steady-state physics running at the mean of the minimum and maximum in both luminosity within $|z|$ <10 cm.

We also highlight that a critical part of the sPHENIX run plan is to have a non-zero crossing angle between the beams – the crossing angle reasoning, implications, and quantitative analysis are in Appendix C. As a change in this BUP compared to previous ones, sPHENIX proposes to run Au+Au collisions at $\theta = 1$ mrad rather than $\theta = 2$ mrad. The larger crossing angle was motivated by the need to significantly decrease the instantaneous luminosity over all z for the TPC while decreasing the luminosity inside $|z| < 10$ cm only modestly. Since the overall projections are now lower, it is likely that the optimum running configuration is at a smaller angle, such as $\theta = 1$ mrad (see Table 2.1 above), but with the specific value to be determined based on continued discussions with C-AD and the TPC sub-system experts.

In the preparation of projections for polarized observables in p+p 2024 running, we use the expected polarization given by the C-AD guidance.

We assume an sPHENIX uptime (i.e. the fraction of time when collisions are available when

Table 2.2: Summary of the sPHENIX Beam Use Proposal for 2024 and 2025, as requested in the charge. The values separated by slashes correspond to different cryo-week scenarios (20/24/28 in 2024 and 24/28 in 2025). The 10%-*str* values correspond to the modest streaming readout upgrade of the tracking detectors.

Species	$\sqrt{s_{NN}}$ [GeV]	Physics Weeks	Min. Bias Rec. Lum. $\lvert z\rvert$ <10 cm	Calo. Trigger Lum. $\lvert z\rvert$ <10 cm
Run-2024, Scenario A, 6 cryo-weeks Au+Au + 20/24/28 cryo-weeks p+p				
Au+Au	200	n/a	n/a (Commissioning running)	
p+p	200	13/17/21	0.34/0.44/0.54 pb^{-1} [@ 5kHz] 2.3/3.1/3.9 pb^{-1} [10%-str]	23/31/39 pb^{-1}
Run-2024, Scenario B, 20/24/28 cryo-weeks p+p + 6 cryo-weeks Au+Au				
p+p	200	9/13/17	0.23/0.34/0.44 pb^{-1} [@ 5kHz] 1.5/2.3/3.1 pb^{-1} [10%-str]	15/23/31 pb^{-1}
Au+Au	200	3	0.4 nb^{-1} (3B events)	not needed
Run-2025, 24/28 cryo-weeks				
Au+Au	200	20.5/24.5	5.2/6.3 nb^{-1} (35B/43B events)	not needed

sPHENIX is taking data with high livetime) of 0.60 for 2024 running since the detector is being commissioned for a new collision systems and new Level-1 triggers are being brought online, rising to 0.80 for subsequent running in 2025. These uptime values fold in the expected livetime of the data acquisition system, which is greater than 90%.

2.2 Proposal for 2024 and 2025

The two-year proposal is summarized in Table 2.2. The numbers separated by slashes correspond to the various scenarios requested in the ALD Charge, with 20, 24, or 28 weeks in 2024 (not counting six weeks of Au+Au carried over from 2023 running) and 24 or 28 weeks in 2025.

2.2.1 Proposal for Run-2024

For the second year of sPHENIX running in 2024, the sPHENIX proposal is to devote every available cryo-week (i.e. except the six weeks allotted for Au+Au running) for p+p collisions with transverse (vertical) polarization. We stress the critical need for high-luminosity p+p reference data for the

sPHENIX physics program. The p+p baseline is the dominant or co-dominant contributor to the statistical uncertainties in many of the unique, flagship sPHENIX measurements such as photon+jet production and Upsilon suppression. In the BUP 2022, the sPHENIX request in a 24-cryoweek p+p/p+Au scenario was 45 pb^{-1} of p+p data, which was the minimum amount needed to provide a QCD vacuum reference for Au+Au collisions, carry out the ColdQCD program, and perform the detailed *in situ* studies of detector performance needed to limit systematic uncertainties. Given the significant reduction in the latest luminosity projections, it will be necessary to have exclusively p+p running for as many cryo-weeks as possible in 2024 to obtain a statistical sample of hard processes on par with that in central Au+Au events (see Chapter 2.4 below).

As part of the 2024 running, it will be necessary to reserve significant time to finish the sPHENIX commissioning process with beam started in 2023. We note that during commissioning, it is necessary for sPHENIX to have complete control over the beam configurations at RHIC, such as by running beams with different fill scheme, aperture, crossing angle, and intensity, to have beams in only one ring of the machine for background studies, etc. Thus, there is no explicit expectation of physics data collected during a cryo-week devoted to commissioning.

The ALD request is to propose a plan which includes a nominal six weeks of Au+Au running in 2024, which we assume includes the necessary cooling, setup, and ramp-up time needed to establish collisions in the system. We note that the choice of optimal plan for these cryoweeks depends on additional information. For example, two elements of RHIC that were incompletely commissioned in Run-23 were the extended EBIS source and the 56 MHz RF system. These directly affect the intensity of the beams and the longitudinal bunch structure (and hence the luminosity drop under different crossing angles). Thus, depending on C-AD guidance over the coming months, information about these elements will impact the placement of Au+Au running within Run-24. For the proposal in this BUP, sPHENIX has prepared two example scenarios corresponding to cases where that running is at the beginning or end of run 2024. There are benefits to either scenario, and we expect that additional information from the continued beam-off commissioning over the next few months can help select which one is the most advantageous. More details about the commissioning status and the needed commissioning tasks with beam for each sub-system are discussed in the accompanying document to this Beam Use Proposal.

In the example where the Au+Au running is at the beginning of run 2024 (Scenario A in Table 2.2), we estimate that the Au+Au running together with four weeks at the start of p+p running would need to be reserved to conclude sPHENIX commissioning, before moving to full high-luminosity physics p+p running. THe specific cryo-week breakdown for this Scenario and the next one is shown in Chapter 2.3. Scenario A has the benefit of the largest number of cryo-weeks available to collect the critical p+p data, but foregoes the opportunity to take Au+Au data in a fully commissioned, physics configuration until 2025.

In the example where the Au+Au running is at the end of run 2024 (Scenario B in Table 2.2), the proposal is to reserve eight weeks at the start of p+p running to conclude sPHENIX commissioning, before moving to p+p physics running and then eventually to six weeks of Au+Au. The benefit of Scenario B is that sPHENIX would take Au+Au data after being fully commissioned, providing a key early look at this collision system before the critical 2025 Au+Au physics run. However, the downside is a potentially decreased efficiency if the Au+Au running, which requires top-energy RHIC operation, is during the summer months.

Scenarios A and B are meant to provide specific quantitative examples for the PAC input. However,

as the run proceeds, depending on RHIC performance and the sPHENIX commissioning progress, we may find that it is advantageous to consider other scenarios, such as: (1) If we start with Scenario B, then in the case of a needed extension of the commissioning period, or lower than expected delivered p+p luminosities, one can choose to continue running p+p during those six reserved cryoweeks. (2) In the case that the budget only allows for a lower number of cryo-weeks (such as 20), we could ask that the six Au+Au weeks be used for more p+p running. (3) We could switch to Au+Au running in the middle of the run to avoid the impact of the high temperatures in the summer, and then back to p+p.

We note that transitioning to p+Au running at any point in 2024 has a significant cost in terms of cryoweeks before there is any appreciable luminosity production. According to the C-AD guidance, this will require 1.5 cryoweeks for moving the DX magnets and machine setup time, and then an expected ramp-up to the projected luminosity production rate. In addition, the p+Au luminosity projections are strongly decreased in the recent guidance update, with overall luminosity production per week down by a factor of two, with another potentially significant factor when one considers a non-zero crossing angle and narrow-vertex collisions. Because of these circumstances, sPHENIX regretfully proposes to defer the envisioned p+Au running, and the Collaboration asks that BNL management continues to search for any possible avenue for high-luminosity p+Au running in the future. We also note that during the 2021 BUP process, when the experiments were asked to consider a shortened running period of only 20 cryo-weeks, the sPHENIX Collaboration chose to eliminate p+Au running entirely to preserve sufficient run time to accumulate needed p+p reference statistics.

2.2.2 Proposal for Run-2025

For the third year of sPHENIX running in 2025, the proposal is to run Au+Au for the entire duration, allowing sPHENIX to accumulate as large a luminosity as possible for the flagship physics program measuring photons, jet, Upsilons, and heavy flavor. For the values in Table 2.2, we used the parameters corresponding to a crossing angle of $\theta = 1$ mrad, which we found can modestly alleviate some of the impact of the decreased luminosity projections. As the understanding of both the RHIC performance and the sPHENIX TPC develop during 2024 run, it is possible that the crossing angle could be optimized further, potentially even with an evolving value over the course of a fill. For the purposes of these projections we further assume, again as a consequence of reduced C-AD projections, that the collision rate will be low enough to allow sPHENIX to record the entire delivered luminosity in purely minimum-bias mode. This assumption will be checked with guidance from C-AD on the expected evolution of the time-dependent instantaneous luminosity at IP8. We note that if the Au+Au rates are unexpectedly higher than these projections and result in a higher than 15 kHz collision rate within the narrow vertex, sPHENIX could use a calorimeter trigger to select high-p_{T} photon events to ensure that the full delivered luminosity is available for this physics channel.

2.2.3 Description of Luminosity Projections

In Table 2.2, the "Min. Bias Rec." luminosity values correspond to events collected via minimum bias triggers that sample a large fraction of the inelastic cross section ($> 90\%$ in Au+Au for example).

These events have collision vertex $|z| < 10$ cm that corresponds to the optimal acceptance range for the full sPHENIX detector, including the inner tracker. For Au+Au collisions, given the updated guidance from C-AD, it is expected that the Au+Au collision rate in the narrow vertex will always be below the upper DAQ bandwidth limit of 15 kHz (except potentially at the very start of a high-intensity store) and thus this captures the full event rate. In p+p collisions, the minimum bias trigger rate will need to be limited below this, with an assumption of 5 kHz in the table, to allow for bandwidth from the calorimeter triggers (below).

As an additional data acquisition method in the 2024 p+p running, the tracking detectors can take data with a partial streaming readout, in which some fixed fraction of the full minimum bias rate (we assume here 10%, labelled "10%-*str*") can be read out with tracking and global detector information only, i.e. without the calorimeters. This option will greatly expand the heavy flavor program, where low-p_{T} states are impossible to select with a calorimeter trigger. Further details on the streaming readout upgrade are given in Appendix D.

The "Calo. Trigger" luminosity values correspond to the total delivered luminosity by RHIC for collisions inside $|z| < 10$ cm. In the p+p running, these will be fully sampled with calorimeter-based fast triggers which are expected to be $> 90\%$ efficient, and all rare events of interest written out. The triggers include those to be used for photon, jet, and Upsilon physics. As a reminder, since in Au+Au running the expected collision rate will always be less than 15 kHz, there is no calorimeter-trigger strategy required (and thus the table is labelled "not needed").

In the next sections, we provide detailed cryo-week breakdowns for each running year, along with explicit assumptions for calculating the recorded and sampled luminosities.

2.3 Cryo-Week Plan

For mapping out a run plan, we state both cryo-weeks for a running period and also physics data taking weeks, i.e. when Physics Running is declared by C-AD. The guidance from C-AD is that there is a 0.5 week "cool down from 50 K to 4 K", then a 2.0 week "set-up mode" for the specific collision species, and then a 0.5 week "ramp-up". If switching species, there is a combined 1.5 weeks for "set-up" and then the physics running begins "with further ramp-up" (not detailed). Lastly, at the end of the running period, there is a 0.5 "warm-up from 4 K to 50 K". In addition, we assume that in the first, second and third weeks of declared Physics Running, one achieves 25%, 50%, and then 75% of the luminosity target, with subsequent weeks at 100%. These are standard assumptions following C-AD guidance.

Following said guidance, we present the cryo-week breakdowns for Scenarios A and B of the sPHENIX proposed 2024 running in Tables 2.3 and 2.4, respectively, and for the proposed 2025 running in Table 2.5.

2.4 Sampled versus Recorded Luminosity

In the Au+Au 200 GeV case, the physics will predominately come from **recorded** minimum bias collisions. This data will be selected by the Level-1 trigger via the MBD that samples approximately

Weeks	Designation
0.5	Cool Down from 50 K to 4 K
2.0	Set-up mode 1 (Au+Au at 200 GeV)
0.5	Ramp-up mode 1 (8 h/night for experiments)
3.0	Outstanding sPHENIX Au+Au Commissioning Time
2.0	Set-up mode 2 (p+p at 200 GeV)
0.5	Ramp-up mode 2 (8 h/night for experiments)
4.0	Dedicated sPHENIX p+p Commissioning Time
13/17/21	Data taking mode 2 (p+p Physics)
0.5	Controlled refrigeration turn-off
20/24/28 (+6 Au+Au)	Total cryo-weeks

Table 2.3: Year 2024 run plan for 20/24/28 (+6 Au+Au) cryo-weeks, Scenario A.

Weeks	Designation
0.5	Cool Down from 50 K to 4 K
2.0	Set-up mode 1 (p+p at 200 GeV)
0.5	Ramp-up mode 1 (8 h/night for experiments)
8.0	Dedicated sPHENIX p+p Commissioning Time
9/13/17	Data taking mode 1 (p+p Physics)
2.0	Set-up mode 2 (Au+Au at 200 GeV)
0.5	Ramp-up mode 2 (8 h/night for experiments)
3.0	Outstanding sPHENIX Au+Au Commissioning Time
0.5	Controlled refrigeration turn-off
20/24/28 (+6 Au+Au)	Total cryo-weeks

Table 2.4: Year 2024 run plan for 20/24/28 (+6 Au+Au) cryo-weeks, Scenario B.

Weeks	Designation
0.5	Cool Down from 50 K to 4 K
2.0	Set-up mode 1 (Au+Au at 200 GeV)
0.5	Ramp-up mode 1 (8 h/night for experiments)
20.5/24.5	Au+Au Data taking (Physics)
0.5	Controlled refrigeration turn-off
24/28	Total cryo-weeks

Table 2.5: Year 2025 run plan for 24/28 cryo-weeks with Au+Au 200 GeV collisions.

90% of the inelastic cross section. For sufficiently high instantaneous luminosities, additional physics may be "sampled" with rare event triggers, for example high-p_T direct photons, where the trigger rejection is very high even in central Au+Au events. However, with the latest guidance from C-AD, it is expected that the entire Au+Au minimum-bias collision rate will be under the 15 kHz DAQ limit and can thus be taken just with MBD triggers. Thus all physics projections are based on the recorded luminosity in Au+Au unless otherwise stated.

In the p+p case, the instantaneous luminosities are sufficiently high that even reading out MBD-triggered events at the upper DAQ bandwidth limit would only yield a small available luminosity for physics measurements. Thus, the physics will predominantly come from **sampled** Level-1 calorimeter-triggered events utilizing photon, electron (e.g. from Upsilon decays), hadron, and jet triggers, the key value is the sampled luminosity for these physics channels. Note that some observables such as lower p_T hadrons (and in particular heavy-flavor hadrons D, Λ_c, B) do not have effective Level-1 physics triggers. Thus, in these cases the recorded luminosity is crucial. We have nominally allocated 5 kHz, out of the 15 kHz Level-1 trigger rate, for p+p minimum bias collection, to collect these events and to understand the performance of the Level-1 calorimeter trigger. A critical addition is the streaming capability for the tracking detectors, which enables much larger minimum bias data sets (without calorimeter readout).

Trigger algorithms have been developed in simulation and tested for p+p running using the EMCal for single photons (typically with p_T greater than 10 GeV) and for electrons (from Upsilon decays typically with p_T greater than 3–4 GeV). In addition, trigger algorithms using the combined EMCal and HCal information have been developed for selecting jets and single hadrons. At the highest p+p interaction rates, rejection factors of order 5000–10,000 are needed to result in a 1–2 kHz bandwidth allocation for a given trigger channel. Full GEANT-4 simulations with HIJING p+p events have been used to document the trigger efficiencies and rejection factors for all Level-1 algorithms. One example set of calculations for jet triggers is shown in Figure 2.1 indicating good efficiency and rejection factors above the required level. The separate commissioning document accompanying this Beam Use Proposal discusses the status of the calorimeter trigger and additional commissioning work needed.

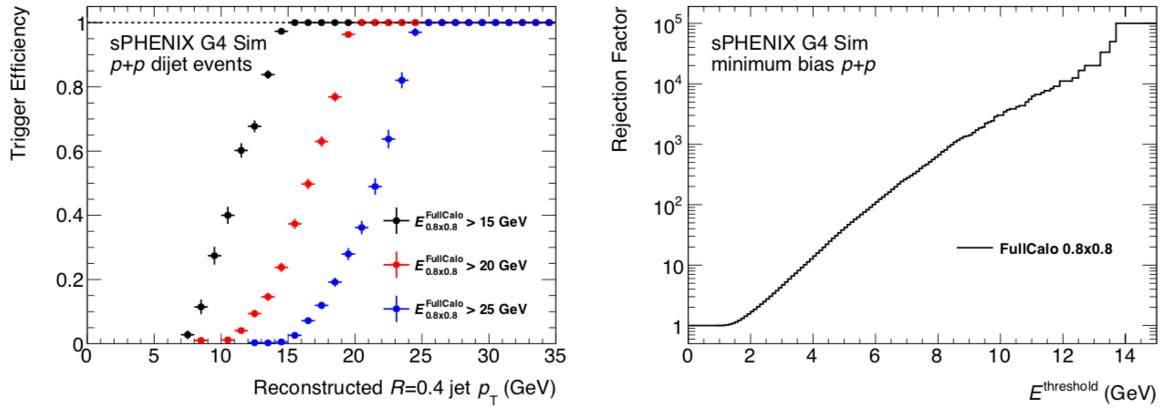

Figure 2.1: sPHENIX full GEANT-4 simulations with HIJING p+p events run through the jet Level-1 trigger emulator with efficiencies (left) and rejection factors (right).

Species	Relevant Luminosity	$\langle N_{coll} \rangle$	Effective-p+p
p+p	39 pb^{-1} (sampled)	1	1.6×10^{12}
Au+Au (min. bias.)	6.3 nb^{-1} (recorded)	250	11×10^{12}

Table 2.6: Comparison of the effective number of p+p collisions from the full data sets from Years 2024 and 2025, assuming the 28 cryo-week scenarios for each. The Au+Au values correspond to the minimum bias case (i.e. all centralities).

Table 2.6 details the number of relevant events recorded or sampled for measuring high p_T jets from running in 2024–2025. For Au+Au minimum bias events, the average number of binary collisions is $\langle N_{coll} \rangle \approx 250$. We note that the Au+Au sample has an equivalent nucleonic luminosity which is an order of magnitude larger than that in p+p collisions. However, since it will be divided into centrality bins and jet quenching will reduce the statistics for all hadronic final states, there is a reasonable balance between the systems. For example, since approximately one third of the nucleon–nucleon luminosity in Au+Au collisions is in the 0–10% events, the ratio of the effective number of p+p collisions between 0–10% Au+Au events and p+p is approximately two to one before jet quenching, and therefore the yields of suppressed final states such as hadrons and jets are expected to be similar.

Chapter 3

Physics Projections

In this Chapter we highlight some of the key physics that sPHENIX will deliver with the run plan in 2024 and 2025 detailed in Chapter 2. **Due to the very recent nature of the August 2023 updates to the luminosity projections from C-AD, the physics projection plots presented in Chapters 3.1– 3.4 are identical to those from the previous year's Beam Use Proposal, and are labelled "BUP 2022".**

A set of statistical projections of physics observables was initially prepared for the sPHENIX Beam Use Proposal in 2020. These have been unchanged for the Proposals submitted in 2021 and 2022, and new projections have been added which use the same luminosity assumptions, since the guidance from C-AD did not substantially change during that time period. In the weeks before the submission of this BUP, the C-AD guidance has changed significantly, regarding the expected luminosity production in both Au+Au (updated C-AD projections August 2023) and p+p (an update around the time of the BUP 2022 submission, and further significant changes in the August 2023 update) running.

Table 3.1 illustrates some example total yields for selected final-state objects above different p_{T} thresholds, given the updated C-AD guidance. However, due the late nature of the updated C-AD guidance, as well as the focus of the sPHENIX collaboration on understanding the commissioning data, the detailed physics projection plots in the sub-sections of this Chapter have not been systematically updated with the latest projected luminosities. Thus, the projection plots below should be understood with the following caveats:

- *Measurements in p+p data.* In the case of Run-24 Scenario A with 28 cryo-weeks, this corresponds to 39 pb^{-1} of sampled and 3.9 pb^{-1} streaming-readout p+p data, compared to the 62 pb^{-1} and 6.2 pb^{-1}, respectively, assumed in BUP 2022. Thus, the expected statistical uncertainties in both calorimeter-triggered (i.e. photons and jets) and MB-triggered (i.e. heavy flavor) observables should be increased by approximately 25%.
- *Most measurements in Au+Au data*, e.g. v_n measurements, or distributions of quantities just in the Au+Au system. For the case of a 28 cryo-week Run-25, this corresponds to 6.3 nb^{-1} of recorded events compared to the 21 nb^{-1} recorded events projected in BUP 2022 for combined 2023 and 2025 running. Thus, the expected statistical uncertainties for these observables should be increased by approximately 80%.

Signal	Au+Au 0–10% Counts	p+p Counts
Jets $p_{\mathrm{T}} > 20$ GeV	6 800 000 ($R_{\mathrm{AA}} = 0.4$)	6 700 000
Jets $p_{\mathrm{T}} > 40$ GeV	20 000 ($R_{\mathrm{AA}} = 0.4$)	19 000
Direct Photons $p_{\mathrm{T}} > 20$ GeV	9 200 ($R_{\mathrm{AA}} = 1$)	3 700
Charged Hadrons $p_{\mathrm{T}} > 25$ GeV	1 300 ($R_{\mathrm{AA}} = 0.2$)	2 600

Table 3.1: Projected counts for jet, direct photon, and charged hadron events above the indicated threshold p_{T} from the sPHENIX proposed 2024 p+p and 2025 Au+Au data taking, with the assumed R_{AA} given for the Au+Au case. These estimates correspond to the 28 cryo-week scenarios, and are based on the latest C-AD guidance from August 2023.

- *Photon and photon+jet measurements in Au+Au.* For these, the plan in BUP 2022 was to use a calorimeter trigger to sample up to 32 nb^{-1} of Au+Au events in Run-23 and Run-25. Thus, for these observables, the expected statistical uncertainties are 140% larger.
- *Ratios between 0–10% Au+Au events and p+p events.* The expected statistical uncertainties are similar between the two systems (see Table 3.1), depending on the particular level of suppression. Thus, one may generally use the impact on the Au+Au data as described above since, except for the direct photon case, that has a similar or worse statistical power as the p+p data.

Finally, while the projections here are focused on statistical uncertainties, we note that in many case large statistics are needed to study systematic effects in data (e.g. isolated track-to-calorimeter matching for inter-detector energy calibration, γ+jet calibration of the energy scale in p+p, etc.), with an impact that is difficult to quantitatively project.

The specific physics projections are split into Section 3.1 (Jet and Photon Physics), Section 3.2 (Upsilon Physics), Section 3.3 (Open Heavy Flavor Physics), and Section 3.4 (Cold QCD Physics). As a reminder, they are not updated from the BUP 2022, and should be understood with the caveats about increased statistical uncertainties given above.

3.1 Jet and Photon Physics

Probing the QGP with precise jet, direct photon, and hadron measurements is a core component of the sPHENIX scientific program. From 2023 to 2025, sPHENIX will collect large data samples to allow for detailed reconstructed jet measurements, including jet yields, di-jet events, jet (sub-)structure and properties, photon-tagged jet quenching measurements, and jet-hadron correlations. The projections in this Section are for light flavor jets; projections for b-quark jet yields and their properties are discussed in Section 3.3.

The projections in this section are based on perturbative QCD calculations previously used in the sPHENIX MIE proposal document [8] applied to the nominal running plan proposed in Section 2.

For p+p collisions, it is has been demonstrated that essentially all photons and jets can be efficiently selected, above a moderate p_{T} value ($\approx$ 20 GeV), by a calorimeter trigger and that the full high-p_{T} charged hadrons yield can be selected indirectly via a jet trigger. For Au+Au collisions, it is assumed that jets and charged hadrons will only be measured in minimum bias events, but that all high-p_{T} photons can be recorded by a dedicated photon trigger in Au+Au data-taking.

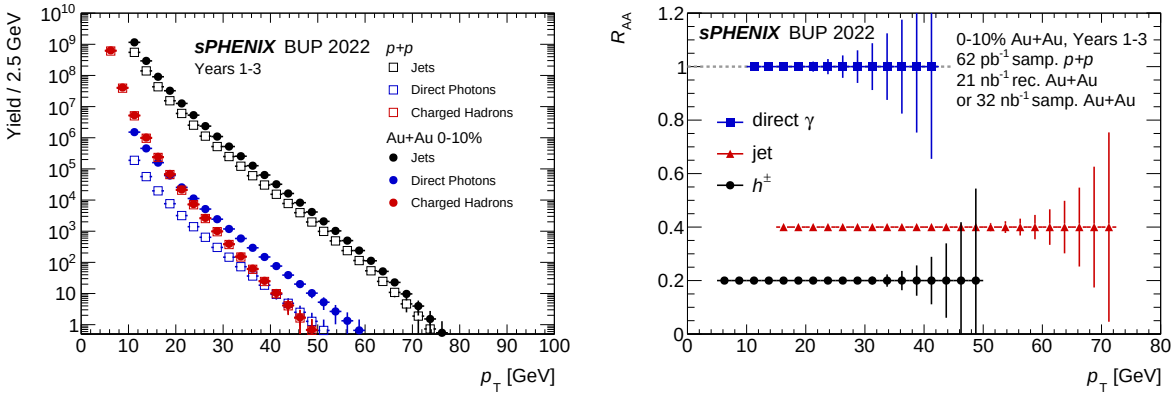

Figure 3.1: Projected total yields (left) and R_{AA} (right) for jets, photons, and charged hadrons in 0–10% Au+Au events and p+p events, for the first three years of sPHENIX data-taking. **Projections shown here use the BUP-2022 luminosity assumptions. See the beginning of Chapter 3 about the qualitative impact of the August 2023 updates to the C-AD projections.**

Figure 3.1 (left) shows the projected total yield of jets, direct photons, and hadrons in p+p collisions and in 0–10% central Au+Au collisions, using a Glauber MC simulation [9] to translate Au+Au event yields to an effective partonic luminosity. Overall suppression factors of $R_{\mathrm{AA}} = 0.2$, 0.4 and 1.0 are assumed for hadrons, jets, and photons in central Au+Au events. In the first three years, sPHENIX will have kinematic reach out to $\sim$ 70 GeV for jets, and $\sim$ 50 GeV for hadrons and photons.

As another way of indicating the kinematic reach of these probes, the nuclear modification factor R_{AA} for each is shown in Figure 3.1 (right). There are varying theoretical predictions concerning the behavior of the R_{AA} at higher p_{T} which will be definitively resolved with sPHENIX data.

The projection plots above indicate the total kinematic reach for certain measurements, such as those which explore the kinematic dependence of energy loss. For other measurements, it is useful to have a large sample of physics objects to study the properties of their intra-event correlations, for example for jets (their internal structure), photons (for photon+jet correlations), and hadrons (for hadron-triggered semi-inclusive jet measurements). We highlight that, in many cases, it is the p+p baseline rather than the Au+Au data will be the dominant contributor to the statistical uncertainties in many of the unique, flagship sPHENIX measurements.

Several specific examples of sPHENIX projections for jet correlations and jet properties follow below.

Figure 3.2 shows a statistical projection of the photon–jet p_{T} balance distribution, and of the sub-jet splitting function z_g, both in p+p events compared to that predicted by the JEWEL Monte Carlo event generator [10] configured for RHIC conditions in 0–10% Au+Au central events. In both cases, sPHENIX will have large-statistics data samples to measure these specific distributions and

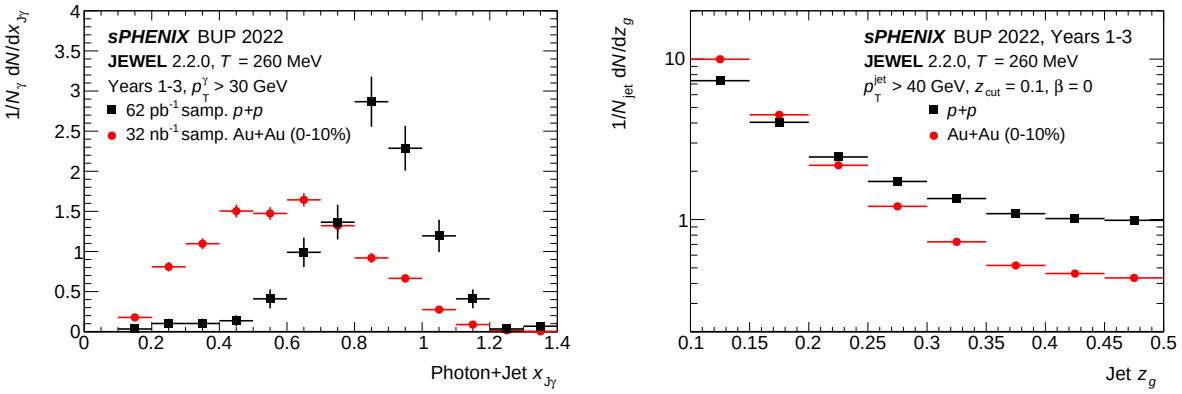

Figure 3.2: Statistical projections for (left) the jet-to-photon p_{T} balance, $x_{\mathrm{J}\gamma}$, for photons with $p_{\mathrm{T}} > 30$ GeV and (right) the subjet splitting fraction z_g for jets with $p_{\mathrm{T}} > 40$ GeV. Statistical uncertainties in the right panel are smaller than the markers. The projected distributions are sampled from those predicted according to JEWEL v2.2.0. **Projections shown here use the BUP-2022 luminosity assumptions. See the beginning of Chapter 3 about the qualitative impact of the August 2023 updates to the C-AD projections.**

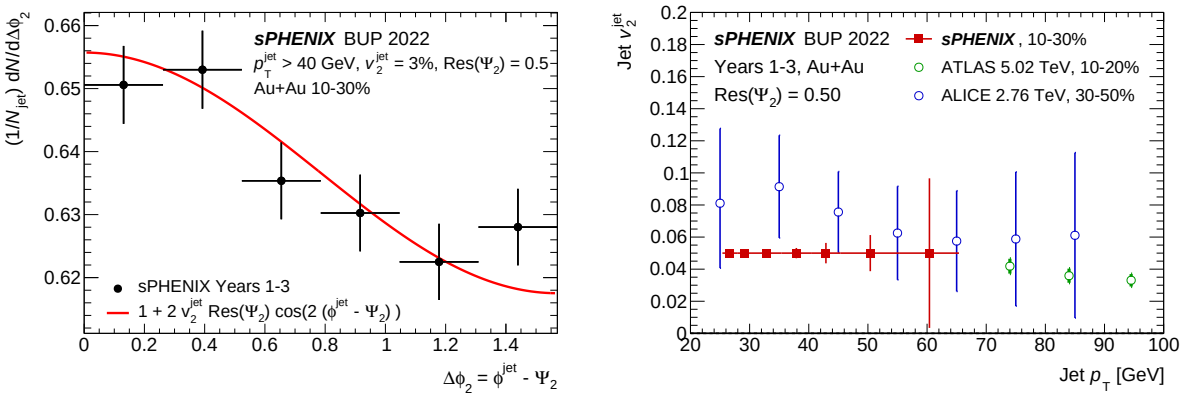

Figure 3.3: Left: Statistical projections for the jet yield as a function of the azimuthal distance from the event plane in 10–30% Au+Au events. Right: Statistical projection for a measurement of the jet v_2 in 10–30% events as a function of jet p_{T}, compared to that from ATLAS and ALICE at the LHC (where the error bars show the total statistical and systematic uncertainties together). **Projections shown here use the BUP-2022 luminosity assumptions. See the beginning of Chapter 3 about the qualitative impact of the August 2023 updates to the C-AD projections.**

investigate the associated physics.

Figure 3.3 which shows a statistical projection for a jet v_2 measurement in 10–30% Au+Au events. The azimuthal dependence of jet quenching is of particular interest since most theoretical calculations have been unable to simultaneously describe suppression and anisotropy at RHIC. The right panel compares the expected kinematic reach with measurements at the LHC by ATLAS [11] and ALICE [12]. Whereas the LHC can achieve a controlled measurement at high p_{T}, the systematic uncertainties grow substantially at lower p_{T}. sPHENIX is expected to have a significant advantage in measuring jets down to lower p_{T} given the lower RHIC energy, and the projection in Fig. 3.3 demonstrates that sPHENIX will have the required luminosity to constrain the jet v_2 in the range

25–60 GeV.

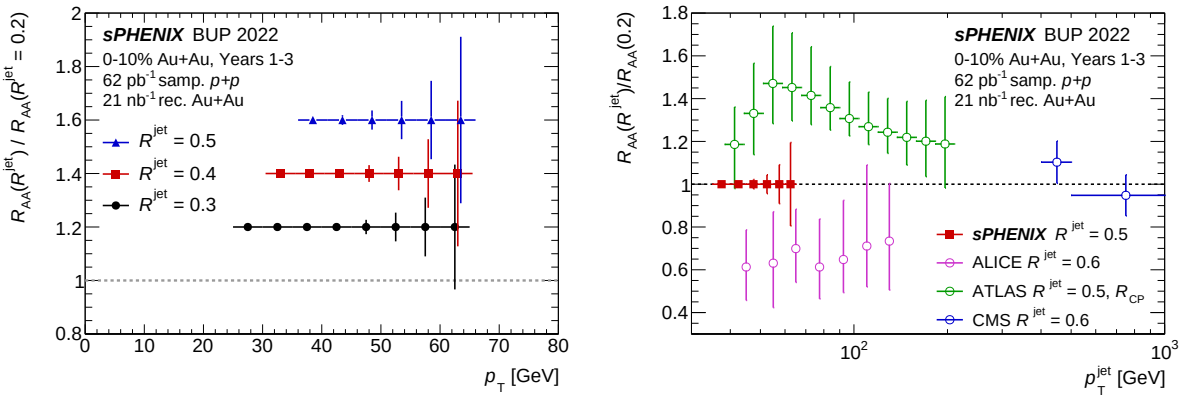

Figure 3.4: Left: Statistical projections for the jet R_{AA} double ratio between a large cone size and that for $R = 0.2$ in 0–10% Au+Au events. Right: Statistical projection for the R_{AA} double ratio for $R = 0.5$ compared to the latest similar measurements at the LHC. **Projections shown here use the BUP-2022 luminosity assumptions. See the beginning of Chapter 3 about the qualitative impact of the August 2023 updates to the C-AD projections.**

Figure 3.4 shows a projection for suppression measurements of large-R jets in sPHENIX. These measurements probe the interplay of out-of-cone energy loss and the angular distribution of medium response effects, most recently highlighted by CMS [13]. For the projection in Figure 3.4, we expect that the jet R_{AA} for different jet R values can be reported in the kinematic region where the jet energy resolution is below 30%. Even with this conservative assumption, sPHENIX will be able to report the R-dependence of the R_{AA} over a wide p_T range and multiple cone sizes. The right panel compares the expected R_{AA} double ratio to the state of the art at the LHC. Note that in the low p_T region, the LHC experiments are in significant tension, with measurements featuring large, model-dependent uncertainties. sPHENIX can make a well-controlled measurement directly in this region of interest.

3.2 Upsilon Physics

High precision measurements of Upsilon production with sufficient accuracy for clear separation of the $\Upsilon(1S, 2S, 3S)$ states is a key deliverable of the sPHENIX physics program. The centrality dependence and particularly the p_T dependence are critical measurements for comparison between RHIC and the LHC, since the temperature profiles from hydrodynamic calculations show important differences with collision energy.

The projected statistical uncertainties for the R_{AA} of all three Y states, including the $\Upsilon(3S)$, are shown in Figure 3.5 (left) as a function of the number of participants in the Au+Au collision. For the $\Upsilon(3S)$ projection, we assume that the R_{AA} for the $\Upsilon(3S)$ is approximately half of that for the $\Upsilon(2S)$, as observed in a recent measurement by CMS at the LHC. Thus, if the relationship between the 2S and 3S is reasonably similar at RHIC, sPHENIX has the opportunity to explore the systematics of the 3S suppression in some detail.

Figure 3.5 (right) shows the projected R_{AA} in 0–60% Au+Au events, as a function of Upsilon

transverse momentum. For comparison, the latest STAR measurement of the 2S+3S together is shown. We highlight that the sPHENIX program offers the unique possibility to observe the strongly-suppressed $\Upsilon(3S)$ state at RHIC energies.

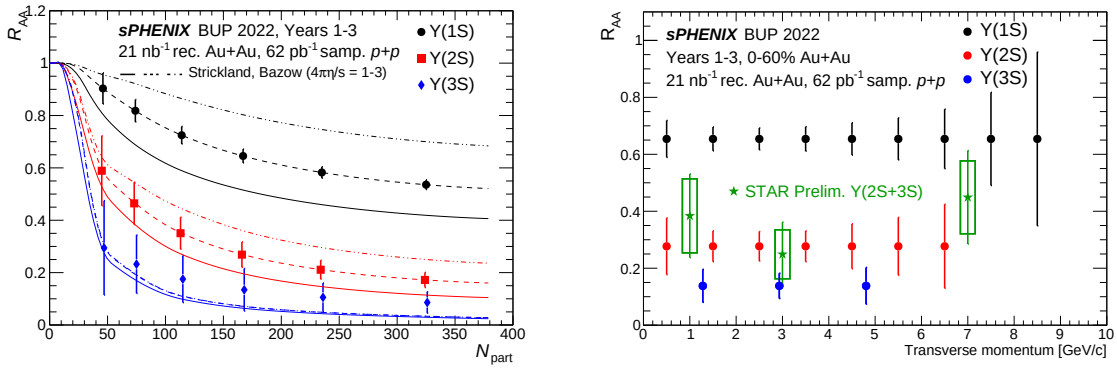

Figure 3.5: sPHENIX projected statistical uncertainties, including the contribution from uncorrelated backgrounds and physics backgrounds (such as from Drell-Yan and $b\bar{b}$), for the Upsilon nuclear modification factors for all three states. Projections for the proposed three-year (2023–2025) run plan are shown as a function of centrality (left) and p_T in 0–60% Au+Au events (right). In the left panel, the $R_{\rm AA}$ for the 1S and 2S is set to the prediction in Ref. [14], while the $R_{\rm AA}$ for the 3S is taken to be half that for the 2S. The right panel includes a comparison to the current best Upsilon suppression knowledge from STAR. **Projections shown here use the BUP-2022 luminosity assumptions. See the beginning of Chapter 3 about the qualitative impact of the August 2023 updates to the C-AD projections.**

The centrality dependence and particularly the $p_{\rm T}$ dependence for all three states are critical measurements for comparison between RHIC and the LHC. Scenarios of melting of the different states at different temperatures must be confronted with data where the temperature profiles from hydrodynamic calculations show important differences with collision energy.

3.3 Open Heavy Flavor Physics

Heavy-flavor quarks (c, b) play a unique role in studying QCD in the vacuum as well as in the nuclear medium at finite temperature . Their masses are much larger than the QCD scale ($\Lambda_{\rm QCD}$), the additional QCD masses due to chiral symmetry breaking, and the typical medium temperature created at RHIC and LHC ($T \sim$ 300–500 MeV). Therefore, they are created predominantly from initial hard scatterings and their production rates are calculable in perturbative QCD. In combination with light sector measurements as discussed in Section 3.1, the large heavy quark mass scale introduces additional experimental and theoretical handles allowing one to study quark-QGP interactions in more detail and to better test our understanding of the underlying physics, including mass-dependent energy loss and collectivity in the QGP. Thus they can be used to study the plasma in a more controlled manner. However, heavy-flavor signals in heavy ion collisions at RHIC energies are relatively rare and current results from RHIC are sparse, particularly in the bottom sector. Improving on these results requires the sPHENIX capabilities of high precision and high data rate.

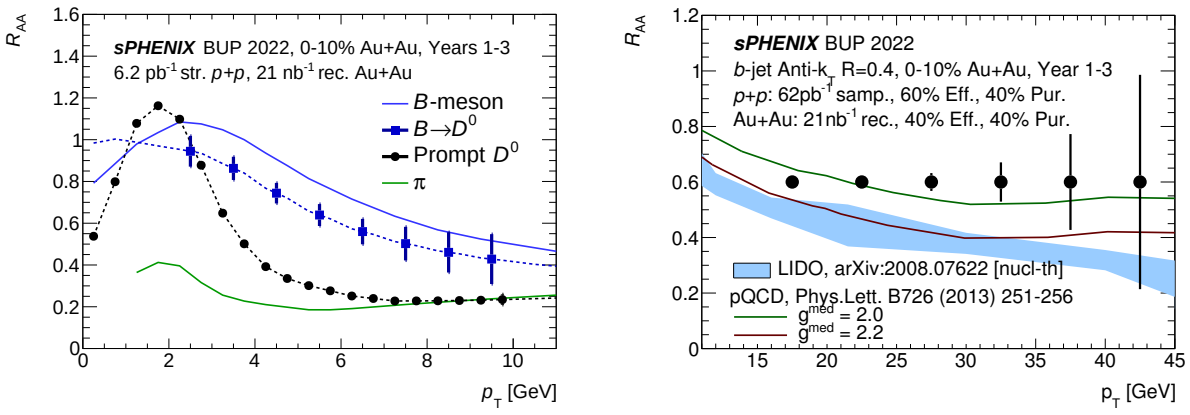

Figure 3.6: Projected statistical uncertainties of nuclear modification factor R_{AA} measurements of non-prompt/prompt D^0 mesons (left) and b-jets (right) as a function of p_T in 0–10% central Au+Au collisions at $\sqrt{s_{NN}} = 200$ GeV from the three-year sPHENIX operation. Left: the solid green curve are averaged R_{AA} for pions and the solid blue line is from a model calculation of R_{AA} for B mesons over several models [15, 16, 17, 18], which maps to the dashed blue line for D-meson from B decay. Right: the curves represents a pQCD calculations with two coupling parameters to the QGP medium, g^{med} [19], and the blue band is from a recent calculation based on the LIDO transport model [20]. **Projections shown here use the BUP-2022 luminosity assumptions. See the beginning of Chapter 3 about the qualitative impact of the August 2023 updates to the C-AD projections.**

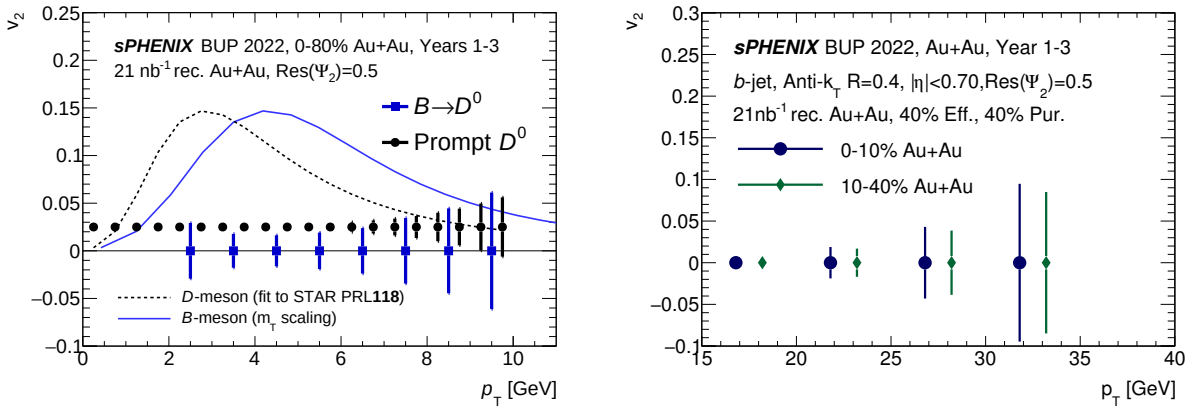

Figure 3.7: Projected statistical uncertainties of v_2 measurements of non-prompt/prompt D^0 mesons (left) and b-jets (right) as a function of p_T in Au+Au collisions at $\sqrt{s_{NN}} = 200$ GeV. Left: the blue dotted line is from best fit of RHIC data, and the black line is for B-meson assuming m_T scaling in v_2. [21, 15, 16, 17] **Projections shown here use the BUP-2022 luminosity assumptions. See the beginning of Chapter 3 about the qualitative impact of the August 2023 updates to the C-AD projections.**

sPHENIX, equipped with a state-of-the-art vertex tracker and high rate streaming DAQ, will bring key heavy-flavor measurements at RHIC fully into the precision era and place stringent tests on models describing the coupling between heavy quarks and the medium. In the first three years of operation, sPHENIX will enable B-meson and b-jet measurements covering the wide transverse momentum range $2 < p_{\mathrm{T}} < 40$ GeV, as shown in Figures 3.6 and 3.7.

The left panel of Figure 3.6 shows the B-meson (D^0 from B) nuclear modification measurements covering the kinematic range $p_T \lesssim 15$ GeV, where nuclear modifications for bottom quarks and light quarks are expected to be quite different, transitioning in the right panel to the b-jet at $p_T > 15$ GeV, where the effect due to the light and heavy quark mass difference is less significant. The current experimental results do not yet confirm the detailed physics behind this transition.

Figure 3.7 (left) shows the elliptic flow v_2 measurements of the charm and bottom meson made with unprecedented precision that offer unique insight into the coupling of the HF quark to the medium. Theoretical modeling using the "Brownian" motion methodology requires that momentum transfer for each interaction is much smaller than the heavy particle mass [22]. It is thus much better controlled for bottom quarks compared to charm quarks [23]. Therefore, precision bottom measurements over a wide momentum range, particularly in the low-p_T region, can offer significant constraints on the heavy quark diffusion transport parameter of the QGP medium along with its temperature dependence. Figure 3.7 (right) shows how the v_2 measurement can be further extended to the tens of GeV range, where the path-length differential energy loss of the b-quark is probed.

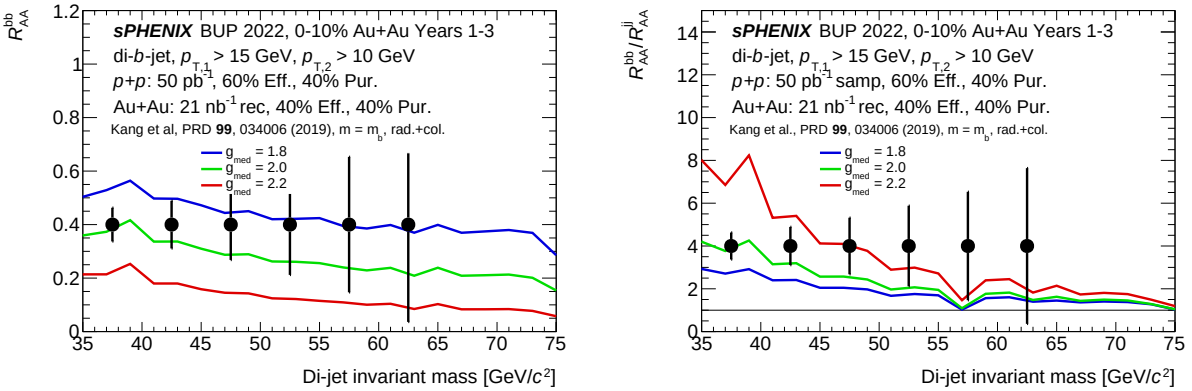

Figure 3.8: Projected statistical uncertainties of nuclear modification for back-to-back b-jet pairs (left) and b-jet-light-jet super-ratio (right) along with pQCD calculations from Ref. [24]. **Projections shown here use the BUP-2022 luminosity assumptions. See the beginning of Chapter 3 about the qualitative impact of the August 2023 updates to the C-AD projections.**

With the large acceptance and multi-observable capability, the sPHENIX experiment is well positioned to explore new heavy-flavor correlations. Recently, the invariant mass of back-to-back heavy-flavor jet pairs has been shown to be a promising experimental observable for studying the propagation of quarks in the QGP [24]. The 3-year projection for the nuclear modification of the invariant mass for back-to-back b-jet pairs and the b-jet-light-jet super-ratio is shown in Figure 3.8. Comparing to predictions based on 10% variation of the coupling parameter, g^{med}, the sPHENIX data will place stringent constraints on the b-quark coupling to the QGP under this model. The large sample for the heavy-flavor hadron and jet also enables a correlation study for heavy-flavor

meson pairs, heavy-flavor meson-jet correlation, and other jet-jet observables that are being studied by the collaboration [25, 26];

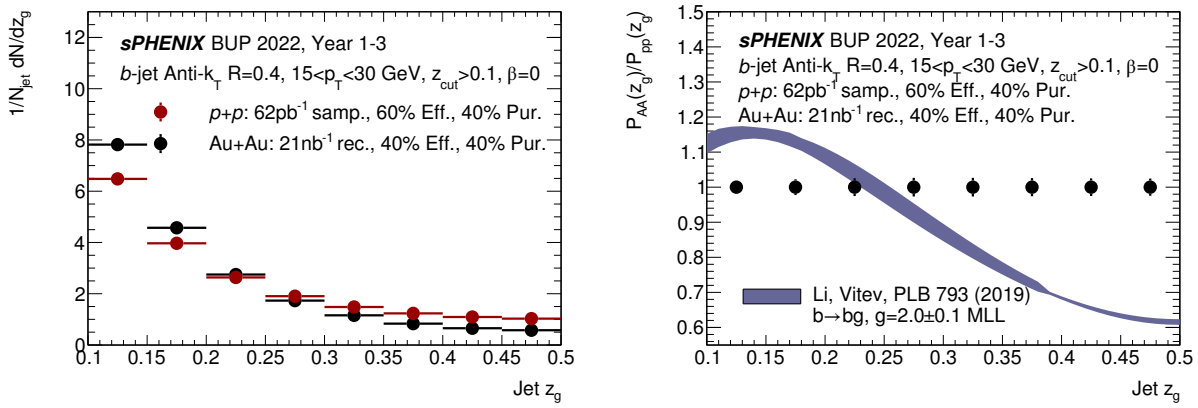

Figure 3.9: Projected statistical uncertainties for the subjet splitting fraction z_g for b-jets in p+p and Au+Au (left) and the Au+Au/p+p ratio compared to the expectation from a pQCD calculations from Ref. [27]. **Projections shown here use the BUP-2022 luminosity assumptions. See the beginning of Chapter 3 about the qualitative impact of the August 2023 updates to the C-AD projections.**

The large yield of identified b-jets will also allow for differential studies of their properties. As one example, the left panel of Figure 3.9 shows the expected statistical uncertainties on a measurement of the sub-jet splitting fraction z_g in 15–30 GeV b-jets in p+p and 0–10% Au+Au events. For this projection, we show only the uncertainty contains statistical uncertainty only and assume a weak correlation between the b-jet tagging efficiency/purity and z_g, while the systematic uncertainty is still under study. The right panel of Figure 3.9 shows the Au+Au/p+p ratio compared to one prediction [27], in which a particularly significant medium modification is expected for b-jets in the unique sPHENIX kinematic region.

Finally, recent RHIC and LHC data indicate significant enhancement of the Λ_c baryon to D^0 meson production ratio in p+p, p+A and A+A collisions [28]. However, the data at RHIC is still sparse and the reference Λ_c/D ratio in p+p collision is missing at RHIC energies, while the current model predictions differ significantly. As shown in Figure 3.10, sPHENIX will enable the first measurement of the Λ_c/D in p+p collisions at RHIC and provide the high precision heavy ion data to quantitatively understand the enhancement of the charmed baryon/meson production ratio and therefore charm hadronization in the QGP.

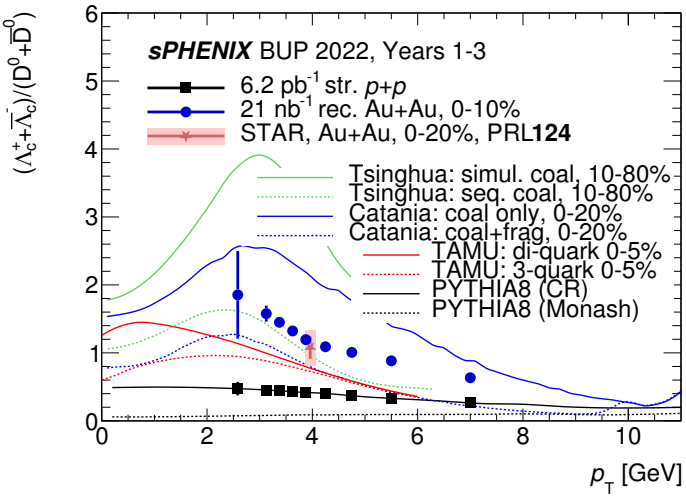

Figure 3.10: Statistical projections of Λ_c/D ratio for both central Au+Au and p+p collisions. This projection is compared with the recent publication from the STAR collaboration in the central Au+Au collisions [28] (red point), model calculations of this ratio in the Au+Au collisions (colored curves), and the PYTHIA8 tunes for the p+p collisions (black curves). **Projections shown here use the BUP-2022 luminosity assumptions. See the beginning of Chapter 3 about the qualitative impact of the August 2023 updates to the C-AD projections.**

3.4 Cold QCD

The sPHENIX detector, primarily designed to study the QGP with jet, photon, and heavy-flavor probes with its trigger and high DAQ rate capabilities, will also provide key opportunities for cold QCD physics measurements with transversely polarized proton beams and studies of transverse-momentum dependent (TMD) effects and hadronization in p+p collisions. We give two particular examples here. Opportunities for measurements in p+Au collisions, including those related to small-system collectivity, are summarized in Appendix B.

In recent years, transverse spin phenomena have gained substantial attention. The nature of significant transverse single spin asymmetries (TSSAs) in hadron collisions, discovered more than 40 years ago at low center-of-mass energy ($\sqrt{s} = 4.9$ GeV), and then confirmed at higher energies up to $\sqrt{s} = 510$ GeV and $p_T \sim 7$ GeV at RHIC, has not yet been fully understood. Different mechanisms have been suggested to explain such asymmetries, involving initial-state and final-state effects, in the collinear or transverse-momentum-dependent (TMD) framework. These descriptions have deep connections to nucleon partonic structure and parton dynamics within the nucleon, as well as spin-momentum correlations in the process of hadronization.

The TSSAs in direct photon and heavy-flavor production probe the gluon dynamics within a transversely polarized nucleon, described by the tri-gluon correlation function in the collinear twist-3 framework, which is connected with the gluon Sivers TMD parton distribution function (PDF), thus far poorly constrained. The Sivers function correlates the nucleon transverse spin with the parton transverse momentum.

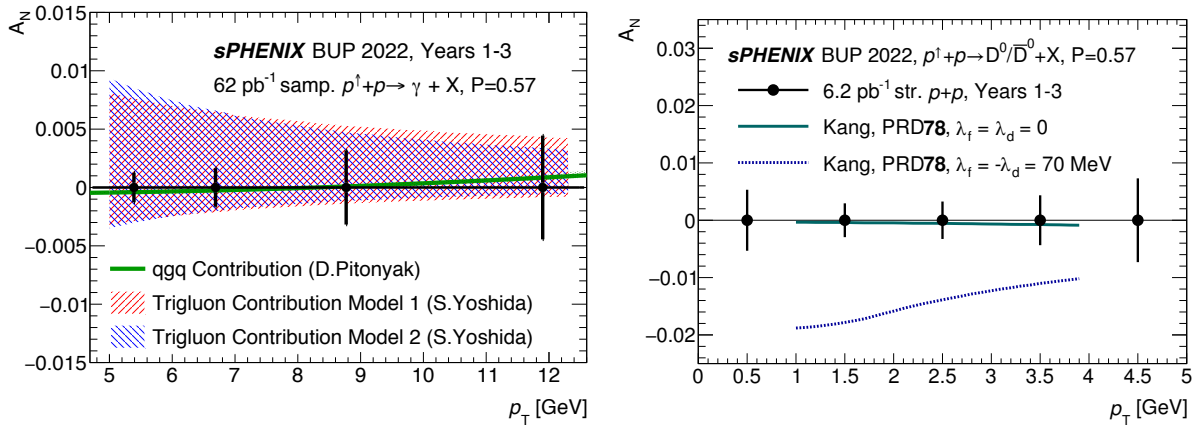

Figure 3.11: Left: Projected statistical uncertainties for direct photon A_N. Right: Statistical projections of transverse spin asymmetry for the D^0 mesons for Year-2, which is compared with various scenarios modeled in the twist-3 model in [29]. **Projections shown here use the BUP-2022 luminosity assumptions. See the beginning of Chapter 3 about the qualitative impact of the August 2023 updates to the C-AD projections.**

The projected uncertainties for the midrapidity direct photon TSSAs compared to theoretical calculations are shown in the left panel of Figure 3.11. The direct photon sample here will be collected with an EMCal-based high-energy cluster trigger. The new capability of the sPHENIX streaming DAQ (detailed in Section D.2) enables a high precision measurement of D^0 TSSA in the mid-rapidity region as shown in the right panel of Figure 3.11.

Another interesting channel related to the Sivers effect is the inclusive jet TSSA, which has not yet been measured at central rapidity. sPHENIX can provide high precision measurements with uncertainties on the level of a few times 10^{-4}. While the opposite sign contribution of up and down quarks to Sivers asymmetry is expected to suppress the measured TSSA, tagging the leading hadron charge will preferentially enhance the contribution from fragmenting up or down quarks, and therefore will enable the flavor-separated measurements in the central rapidity kinematics. Such measurements are complementary to the future jet TSSAs at the EIC, and are also expected to have opposite signs due to the properties of the gauge links involved in the processes. This provides a fundamental test of QCD factorization in $p+p$ and $e+p$ interactions.

Dijet measurements allow for direct access to parton intrinsic transverse momentum k_{T}. Again, charge-tagged jets will enhance the effect from either up or down quarks, which otherwise will be essentially cancelled out. Recent STAR preliminary results showed a nonzero effect for charge-tagged jets. As a dedicated detector for jet and photon measurements, sPHENIX is expected to significantly contribute to dijet measurements, and to extend them to photon-jet measurements which can isolate the quark-gluon scattering process at leading order, thus giving access to the gluon Sivers effect.

Another possible origin of the observed TSSAs is the Collins mechanism, which correlates the transverse polarization of a fragmented quark to the angular distribution of hadrons within a jet. This gives access to the transversity distribution in the proton, which can be interpreted as the net transverse polarization of quarks within a transversely polarized proton. Along with the unpolarized PDF and helicity PDF, transversity is one of three leading-twist PDFs, least known at

the moment. The integral in x over the valence quark transversity distribution defines the tensor charge, a fundamental value calculable in lattice QCD, therefore enabling the crucial comparison of experimental measurements with *ab initio* theoretical calculations. Unlike semi-inclusive DIS measurements on the proton, p+p collisions are more sensitive to the d-quark transversity and its tensor charge.

Measuring angular distributions of dihadrons in the collisions of transversely polarized protons, couples transversity to the so-called "interference fragmentation function" (IFF) in the framework of collinear factorization. The IFF describes a correlation between the spin of an outgoing quark and the angular distribution of a hadron pair that fragments from that quark. A comparison of the transversity signals extracted from the Collins effect and IFF measurements will explore questions about universality and factorization breaking.

The first non-zero Collins and IFF asymmetries in p+p collisions have been observed by the STAR collaboration at midrapidity [30, 31] and shown to be invaluable to constrain the transversity distribution. sPHENIX, with its excellent hadron and jet measurement capabilities, is expected to deliver high-statistics samples for both Collins and IFF asymmetries over a broad kinematic range. We note that the capability to collect a significant data sample with streaming readout and with calorimeter triggers will allow for precise measurements in the low- and high-x ranges, respectively.

Chapter 4

Summary

sPHENIX is the first new collider detector at RHIC in over twenty years, capable of performing high-precision studies of jet production, jet substructure, and open and hidden heavy flavor over an unprecedented kinematic range at RHIC. The experiment is a specific priority of the DOE/NSF NSAC 2015 Long Range Plan and will play a critical role in the completion of the RHIC science mission by enabling qualitatively new measurements of the microscopic nature of Quark-Gluon Plasma. sPHENIX is distinguished by high rate capability and large acceptance, combined with high precision tracking and electromagnetic and hadronic calorimetry.

The construction and installation of the experiment has successfully concluded, with major progress towards the commissioning all subsystems of the detector with beam performed during the 2023 run. The sPHENIX experiment will finish commissioning and take first physics data in 2024, with 2025 foreseen as the final year of sPHENIX operations as dictated by BNL's reference schedule for the EIC project.

The two remaining runs play a critical role in fulfilling the sPHENIX science mission outlined in the NP Long Range Plan:

- Year-2 will see the successful conclusion of detector commissioning, as well as the accumulation of high-statistics transversely polarized $p+p$ data. This dataset will be crucial for providing the physics reference for studies of the Quark-Gluon Plasma, for exploring the structure of the proton through the ColdQCD program, and for serving as an important dataset for *in situ* studies of the detector performance.
- Year-3 is focused on collecting a very large statistics Au+Au data set for measurements of jets and heavy flavor observables with unprecedented statistical precision and accuracy.

The sPHENIX collaboration, comprising 360 scientists from 82 institutions from 14 countries, is excited for the unique physics opportunities enabled by this run plan and to positively conclude the scientific mission of RHIC.

Appendix A

Beam Use Proposal Charge

The updated charge from the Associate Laboratory Director Haiyan Gao was received by the sPHENIX Spokespersons in August 2023. The charge is included below.

```
STAR: Beam Use Requests for Runs 24-25
sPHENIX: Beam Use Requests for Runs 24-25

The Beam Use Requests should be submitted in written form to PAC by August 25, 2023
by emailing Fran and copy me and John the BUR directly or provide a link to access
the BUR before the due date.

The BURs should be based on the following number of cryo-weeks. For Run 2024, we
ask that you consider three scenarios for 20, 24 and 28 cryo-weeks each, given the
uncertain budgetary situation. Additionally due to the recent Blue Ring valve box
event, we ended Run 2023 in August so six Au+Au weeks from Run 2023 will be carried
forward into Run 2024

For Run 2025, the first number is the proposed RHIC run duration for scenario 1 and
the second number corresponds to optimal duration (scenario 2) presented to the
DOE-ONP in BNL's FY25 Lab Managers' Budget Briefing:

2024:  20/24/28 + six weeks of Au+Au
2025:  24 (28)
```

Appendix B

Physics opportunities with p+Au running in sPHENIX

Note: The quantitative details in this appendix have not been updated to reflect the latest available C-AD guidance for p+p and p+Au running from August 2023. It is included here for archival reasons to give an illustration of the sPHENIX physics possibilities for RHIC p+Au running.

B.1 Transverse Spin: $p+p$ vs $p+A$

Unique opportunities are present with polarized $p^{\uparrow}$+A collisions at RHIC to study spin effects in a nuclear environment. These studies provide new insights into the origin of the observed TSSAs and a unique tool to investigate the rich phenomena behind TSSAs in hadronic collisions. TSSAs measured in polarized $p^{\uparrow}$+A collisions moreover offer a new approach to studying small-system collisions, in which numerous surprising effects have been observed in recent years.

First RHIC results from the 2015 RHIC run showed a puzzling evolution of the TSSA from $p^{\uparrow}+p^{\uparrow}$ to $p^{\uparrow}$+Al and then $p^{\uparrow}$+Au. While STAR's preliminary result for π^0 asymmetry in forward rapidity (with $0.2 < x_F < 0.7$) showed no significant nuclear dependence, PHENIX's positively charged hadron asymmetries in the intermediate rapidity range (with $0.1 < x_F < 0.2$) discovered a strong nuclear dependence in the TSSA, from $A_N \sim 0.03$ in $p^{\uparrow}+p^{\uparrow}$ collisions to a value consistent with zero in p+Au collisions. No clear explanation for such a behavior has been offered at the moment. Obviously, more data, differentiated in p_T and x_F, would be highly desirable. sPHENIX is able to collect much more data in this channel, with fine binning, which is expected to provide crucial information on the nature of TSSAs in hadronic collisions and on understanding of the spin probe—nucleus interaction, a novel topic directly associated with RHIC's unique ability to collide polarized protons with nuclei.

The left panel Figure B.1 shows the projected uncertainties for sPHENIX, based on minimum bias data collected with the streaming readout. The sPHENIX tracking system will provide us with charged hadron measurements in the pseudorapidity range up to $\eta = 2$, which overlaps with the PHENIX range, where the strong nuclear effect was observed ($1.2 < \eta < 2.4$).

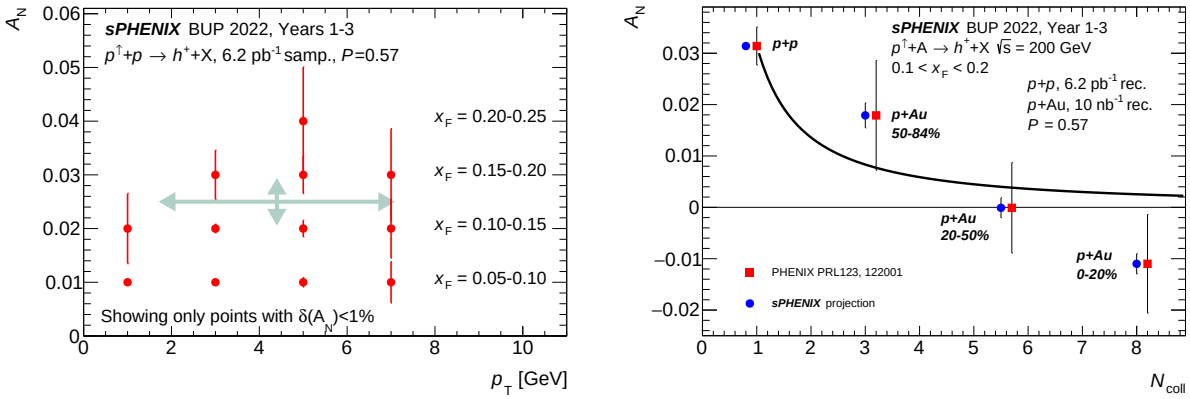

Figure B.1: (Left) Projected statistical uncertainties for h^+ A_N in p+p collisions, for data collected with streaming readout; green arrows indicate the statistical uncertainty and p_T coverage of the single PHENIX data point (with $0.1 < x_F < 0.2$). (Right) Projected statistical uncertainties as a function of the average number of nucleon-nucleon collisions in each centrality bin.

In addition, sPHENIX can explore the nuclear dependence of TSSAs. The first RHIC p+Al and p+Au runs with transversely polarized protons in 2015 brought a number of surprising results, among them the strong nuclear suppression of the charged hadron TSSA in p+Au collisions compared to p+p collision in the intermediate rapidity region of $\eta = 1.2 - 2.4$ [32], discovered by PHENIX, while more forward measurements of π^0 TSSA, as reported by STAR, showed only weak nuclear dependence [33]. Such behavior of TSSA in p+Au collisions remains unexplained. The data to be collected by sPHENIX in p+p and p+Au collisions would considerably improve the precision of the measurements, as shown in the right panel of Figure B.1. By allowing for a measurement of TSSAs with fine binning in p_T and x_F in extended ranges, these would provide valuable information for studying rich phenomena behind TSSA in hadronic collisions, and utilize RHIC's unique capabilities to collide high energy polarized protons and heavy nuclei.

Other measurements (e.g. Collins and IFF asymmetries) will also be compared between p+p and $p^{\uparrow}$+Au systems and may bring new surprises.

B.2 Unpolarized Measurements

A number of measurements that do not require beam polarization are planned in p+p and p+A collisions. Figure B.2 demonstrates the kinematic reach for inclusive jet, photon, and charged hadron measurements in this system via the expected total yields and the projected uncertainties in the nuclear modification factor $R_{p\mathrm{A}}$. sPHENIX will deliver sufficient data to measure jets out to $\sim$ 70 GeV, and charged hadrons and direct photons out to $\sim$ 45 GeV.

Hadronization studies will be performed with hadron-in-jet measurements, multi-differential in momentum fraction z of the jet carried by the produced hadron, in the transverse momentum j_T of the hadron with respect to the jet axis, and in the angular radial profile r of the hadron with respect to the jet axis. This includes studies for both light quark and heavy quark hadrons. Comparison of p+p and p+A collisions will provide information on the nuclear modification of hadronization

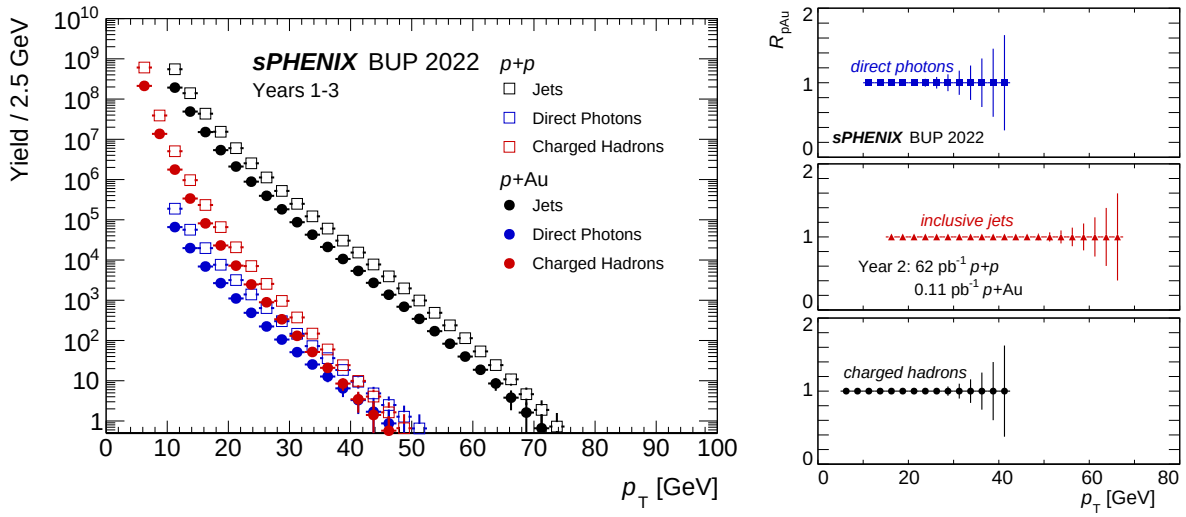

Figure B.2: Projected total yields (left) and R_{pA} (right) for jets, photons, and charged hadrons in centrality-integrated p+Au events, for the first three years of sPHENIX data-taking.

processes. Measurements performed by PHENIX of non-perturbative transverse momentum effects and their nuclear modifications in back-to-back dihadron and photon-hadron correlations, will be extended to dijet and photon-jet measurements in sPHENIX. These measurements will help to separate the effects associated with intrinsic parton momentum k_T in the nucleon or nucleus and fragmentation transverse momentum j_T. These correlation measurements may also help to probe theoretically predicted factorization breaking effects within the transverse-momentum-dependent framework. Upsilon and J/ψ polarization measurements will shed further light on heavy quarkonium production mechanisms.

B.3 Collective behavior in p+A collisions

Over the last decade one of the exciting areas of heavy ion physics relates to collectivity in small systems – see Ref. [34] for a recent review. In p+p and p+Pb collisions at the Large Hadron Collider (LHC) and p+Au, d+Au, ^{3}He+Au collisions at RHIC, there is strong evidence for the translation of initial geometry deformations in flow harmonics.

Correlations with light particles. Using the 10%-streaming readout, even a modest p+Au run would provided enormous statistics for track-only analyses. As an example of what this provides buys, Figure B.3 shows the projected statistical uncertainties for the elliptic flow cumulants in p+Au collisions as a function of track multiplicity. For the 0-5% most central selection, one would have precision measurements up through the 8th order cumulant. These measurement can provide qualitatively new insights on multi-particle collectivity that are hinted at via the PHENIX published d+Au cumulants, with second, fourth, and very modest sixth orders [35].

Additionally, the PHENIX published results in Nature Physics [36] on elliptic and triangular flow have generated significant interest in the field, which have now been corroborated with additional analysis checks [37]. There have since been multiple STAR preliminary results that generally

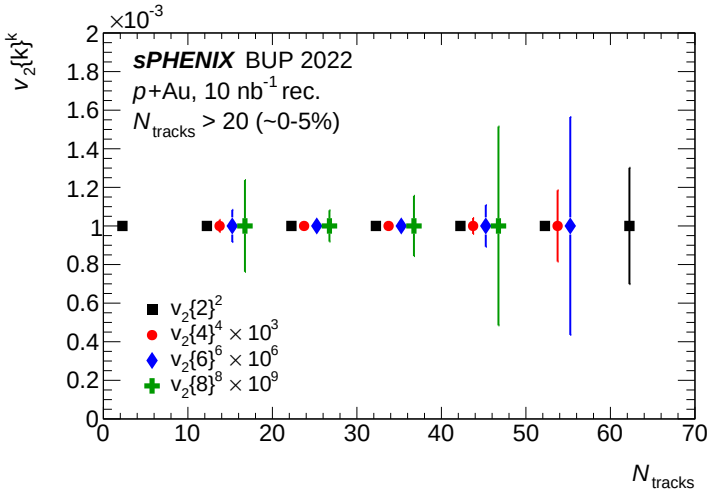

Figure B.3: Projected statistical uncertainties for charged hadron cumulants up to eighth order. These results are obtainable in the 24 and 28 cryo-week scenarios.

confirm the elliptic flow but have a significantly different result for triangular flow in p+Au and d+Au collisions. While publication of the STAR results would be a positive step forward, a parallel way to proceed would be to measure both short-range and long-range correlations in the same experiment with high statistics. sPHENIX will have the same tracking coverage as the STAR barrel detector and a p+Au run would result in much higher statistics data samples. The sPHENIX Event Plane Detector (recently awarded an NSF MRI and under construction) enables PHENIX-style long-range correlations as well. Thus, this p+Au data set in sPHENIX is likely to further elucidate collectivity in small systems and the relevant sub-nucleon geometry.

Heavy flavor collectivity. Heavy flavor (charm and bottom) quarks are an excellent probe of QGP effects. Once produced in early high-Q^2 processes, the flavor is conserved and thus the quarks get dragged and diffused through the medium. Measurements of charm and bottom hadrons and bottom-tagged jets in Au+Au collisions comprise a major part of the sPHENIX program as detailed in Section 3.3. Recent measurements of collectivity in small systems has increased the focus on measurements of these heavy quarks in p+Au and p+Pb collisions at RHIC and the LHC. Measurements of significant D meson elliptic flow v_2 in p+Pb collisions by CMS at the LHC [38] is intriguing since the transverse momentum distribution appears mostly unmodified relative to p+p collisions [39]. Even muons from charm decays have a significant v_2 in high multiplicity p+p collisions at the LHC, though muon from bottom decays are consistent with zero [40].

sPHENIX can make comparable precision measurements in a p+Au run of both the transverse momentum spectrum and the elliptic flow. As an example, the left panel of Figure B.4 shows the projected statistical uncertainties for fully-reconstructed prompt D^0 meson v_2 as a function of transverse momentum from a 2024 p+Au run, compared to the previous measurement in d+Au collisions with PHENIX, and the measurement by CMS. Measurements at both RHIC and the LHC are important to constrain explanations for these anisotropies.

Jets and high-p_T hadrons. A critical baseline for understanding jet quenching effects in nucleus-nucleus collisions is to measure the same observables in p+Au collisions. Originally back in 2003, the d+Au run was motivated by the desire to isolate so-called "cold nuclear matter" effects from jet

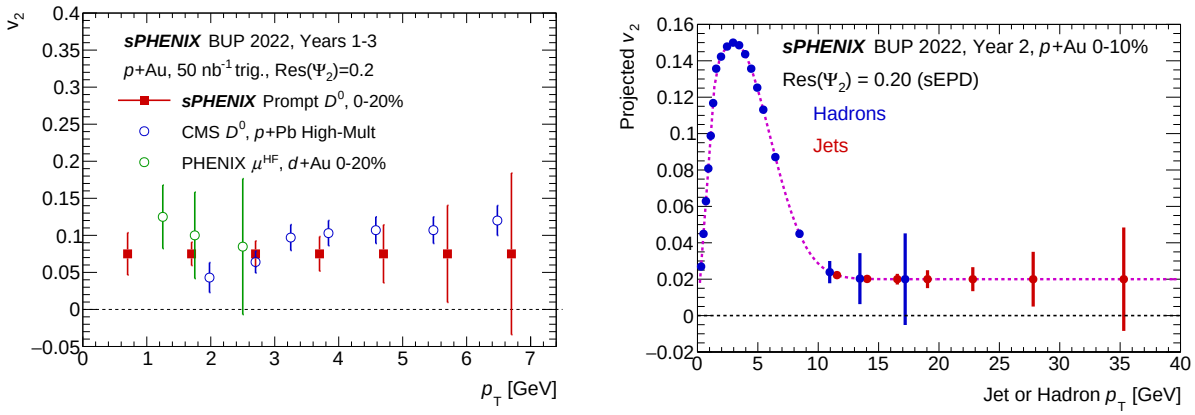

Figure B.4: Left: sPHENIX projected statistical uncertainties for fully-reconstructed prompt D^0 meson v_2 as a function of transverse momentum in p+Au 0-20% central collisions, compared to v_2 for heavy flavor muons from PHENIX and D^0's from CMS [38]. Right: Projected sPHENIX statistical uncertainties for charged hadron and reconstructed jet v_2 versus p_T in 0-10% central p+Au collisions.

quenching. Since then, the measurements have taken on the additional burden of trying to cleanly identify potential jet quenching effects in small collision systems.

The ATLAS experiment at the LHC has measured elliptic flow coefficients v_2 for charged hadrons in the high p_T region 10–50 GeV in p+Pb collisions [41], with a quantitatively similar p_{T} dependence to this same region in Pb+Pb collisions. In Pb+Pb collisions this azimuthal anisotropy is thought to result from differential jet quenching with respect to the collision geometry. However, currently no jet quenching is observed in p+Pb collisions, and so this is challenging as a common explanation in p+Pb. sPHENIX will be able to measure elliptic flow coefficients for charged hadrons and reconstructed jets up to high p_T, as shown in the right panel of Figure B.4. As part of a suite of p+Au hard process measurements by sPHENIX, one will have excellent constraints on explanations of this phenomena.

Appendix C

Crossing Angle

Note: The quantitative details in this appendix have not been updated to reflect the latest C-AD guidance for p+p, p+Au, and Au+Au running released in August 2023. It is included here for archival purpose and to illustrate the relevant issues. The sPHENIX Collaboration is in communication with C-AD to obtain or produce updated versions of these Figures, which may impact the particular fill/crossing angle strategy needed to optimize the delivered luminosity within the narrow vertex range.

The original C-AD projections for Au+Au 200 GeV collision rate as a function of time-in-store for the years 2023, 2025, and 2027 are shown in Figure C.1 (left). The black curves are the collision rate for interactions at any longitudinal z vertex position, while the red curves are the collision rate for interactions with $|z|$ <10 cm. The magenta curve corresponds to the design specified 15 kHz sPHENIX Level-1 trigger accept rate. These projections are with zero crossing angle between the beams.

The sPHENIX optimal acceptance for the inner tracking detectors is with collisions within $|z|$ <10 cm. Thus, it is clear that a majority of the collisions in this running mode with zero crossing angle have highly sub-optimal tracking acceptance. In principle these collisions far outside the optimal region (i.e. $|z| > 10$ cm) still could be used for calorimeter-only physics measurements (e.g. high p_T photons and calorimetric jets) – however, one would not have good acceptance to measure jet fragmentation functions, or medium response via tracks in these events. There is a significant down side to the very large collision rate outside of $|z|$ <10 cm. These collisions still leave hits in the TPC and thus substantially increase ion back-flow (IBF) and fluctuations in the IBF. This additional charge is corrected for but at the same time gets more and more challenging and eventually degrades the track momentum resolution and track finding efficiency. Additionally, components of sPHENIX including the calorimeter silicon photo-multipliers (SiPMs) are susceptible to radiation damage over time. These additional collisions significantly increase the overall time-integrated radiation load on the detector.

Therefore, after detailed discussions with C-AD, sPHENIX plans to run with a nominal beam crossing angle of 2 milliradians in Au+Au collisions. C-AD has included collision rate information at beam crossing angles of 0, 1, and 2 milliradians in their projections document. Figure C.1 (right) shows the collision rate as a function of time in store for a nominal 2 milliradian crossing angle. There is a modest reduction in collision rate within $|z|$ <10 cm; however, it still exceeds the 15 kHz

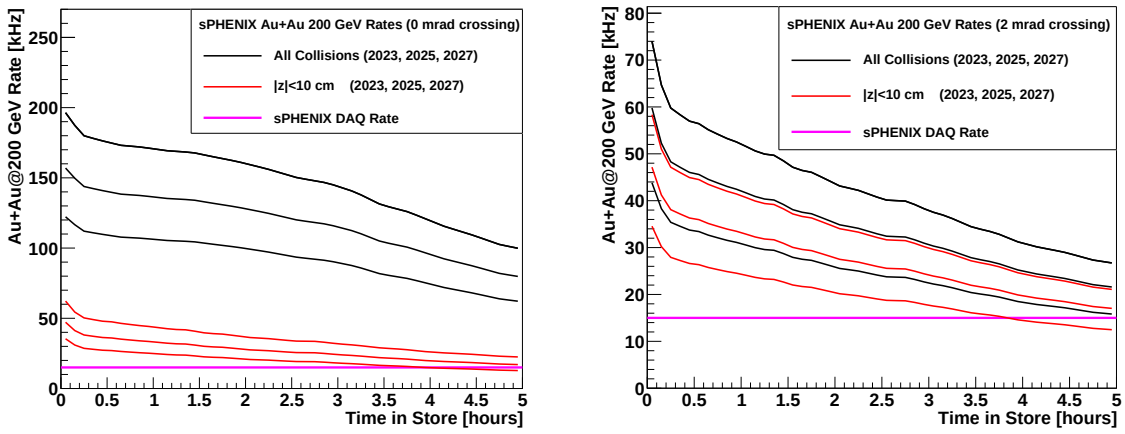

Figure C.1: (left) Estimated Au+Au at 200 GeV collision rate as a function of Time in Store for all collisions (black) and collisions within $\pm$ 10 cm (red). The bottom to top set of curves in each color are for the C-AD projections in their document corresponding to 2023, 2025, 2027. Also shown as a magenta line is the sPHENIX data acquisition rate of 15 kHz for reference. These projections are with zero crossing angle between the beams. (right) The same calculated quantities are shown for a 2 milliradian crossing angle between the beams.

Level-1 accept rate throughout the store. What is most noticeable is the reduction by almost a factor of three in total collision rate. This effectively translates into a factor of three lower radiation load on the detector and three times lower charge deposition in the TPC. Small optimizations around the 2 milliradian value may be possible; for the purposes of this document we have consistently used this 2 milliradian crossing angle for all projections.

Similar issues of acceptance and radiation load / IBF have to be balanced for p+p and p+Au running. The current proposal is to run with the same 2 milliradian crossing angle for these systems as well. We highlight that in p+p and p+Au running, the larger collision rate with lower track multiplicities may lead to small IBF fluctuations since the collisions are spread out in z vertex and there are more random chances to average out relative to a smaller number of Au+Au collisions with highly variable multiplicity. It may be that there is thus a somewhat smaller crossing angle that will be optimal for the smaller collision systems.

C.1 Summary of Projected Luminosities

Wolfram Fischer and C-AD have provided a MATHEMATICA notebook for estimating the collision rate and z-vertex collision distribution as a function of beam crossing angle. After confirming values with C-AD, we include the generated set of results here for completeness, see Figures C.2, C.3, and C.4.

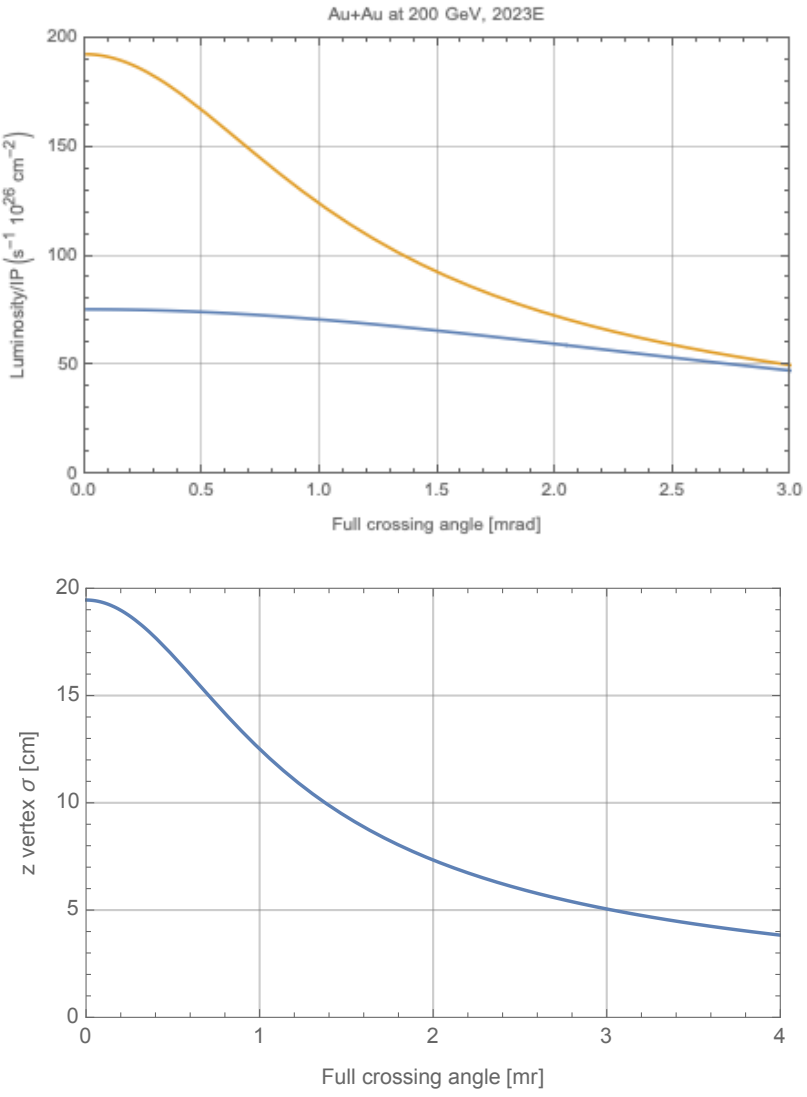

Figure C.2: C-AD MATHEMATICA file generated Au+Au collision luminosity (left) and z-vertex Gaussian σ (right) as a function of beam crossing angle.

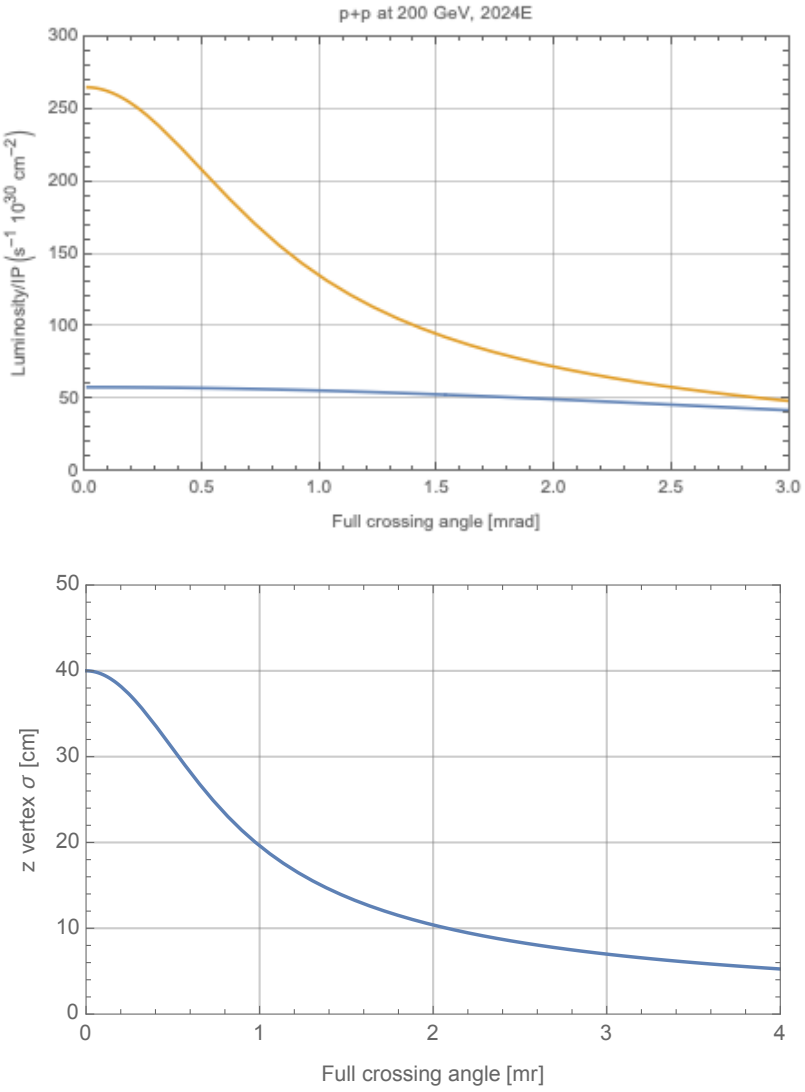

Figure C.3: C-AD MATHEMATICA file generated $p+p$ collision luminosity (left) and z-vertex Gaussian σ (right) as a function of beam crossing angle.

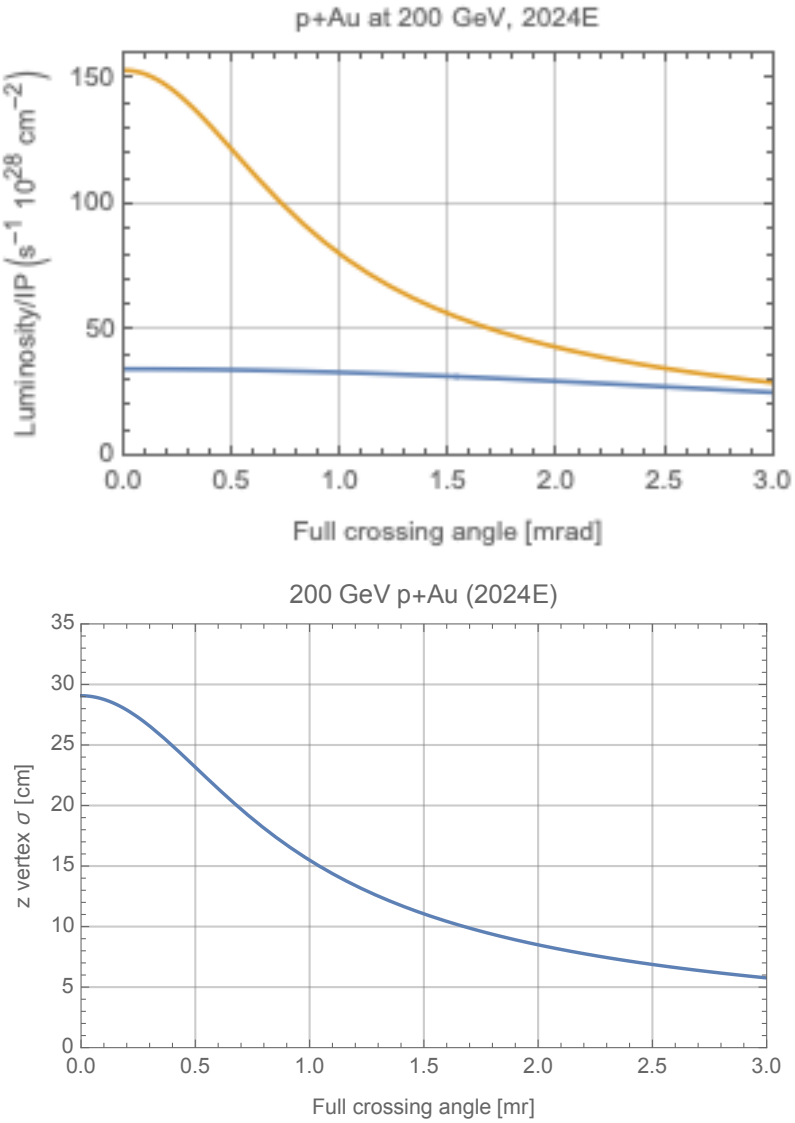

Figure C.4: C-AD MATHEMATICA file generated p+Au collision luminosity (left) and z-vertex Gaussian σ (right) as a function of beam crossing angle.

Appendix D

Upgrades of the sPHENIX Readout

Note: The quantitative details in this appendix have not been updated to reflect the latest C-AD guidance, cryo-week request, or detector development status. It is included here for archival reasons. The commissioning summary document which accompanies this Beam Use Proposal provides the latest information on the status of the streaming readout.

In this appendix we detail the potential of two modest cost upgrades of the sPHENIX data acquisition and readout system to significantly enhance the original physics program. The first is a streaming (rather than triggered) readout of the tracking detectors (MVTX, INTT, and TPC) which could be available at 10% capacity for the 2024 run and at 100% capacity for running in 2026–2027 should that opportunity arise. The second is a demultiplexing of the readout electronics for the calorimeter system which would enable a doubling of the Level-1 trigger rate for these detectors from 15 kHz to 30 kHz. This upgrade could be available for running in 2026–2027. We detail these two options in the sections below.

D.1 Streaming Readout Upgrade for the sPHENIX Trackers

The nominal sPHENIX DAQ model assumes calorimeter-based Level-1 triggers for $p+p$ and $p+$Au data taking. Many sPHENIX observables, such as photons and jets, leave clear signatures in the calorimeter system that can be used to produce a sufficiently selective Level-1 trigger. However, further physics opportunities are present only in the non-triggerable data stream. One example is low-p_T open heavy-flavor hadrons that decay hadronically and leave relatively small signals in the calorimeters compared to the background coming from the underlying event. These physics channels cannot be efficiently collected via calorimeter triggers, which have too high an energy threshold. One would likely allocate 1-5 kHz of the full 15 kHz of the sPHENIX trigger bandwidth for this type of program in minimum bias $p+p$ or $p+$Au. This translates into rather limited statistics for these rare low-p_T heavy-flavor signals as quantified in Table D.1 (left column).

The tracking detectors for the sPHENIX experiment all support streaming readout mode, that is where the digitization and readout of the data off the detector does not require Level-1 trigger information as shown in Figure D.1. The currently envisioned nominal data taking mode is where the data acquisition selects the time-slice of the tracker data that corresponds to the calorimeteric-

triggered event and saves those time-slices to the output raw data file. A streaming readout upgrade in the data acquisition (DAQ) firmware and software is being developed by the collaboration to record a tunable fraction of the tracker data stream on top of the calorimeteric-triggered events, which can vastly increase the fully recorded minimum bias collision event in the full tracking system.

This hybrid trigger-streaming DAQ is particularly efficient in the sense that the number of recorded events per gigabyte of raw data is optimized. By extending the tracker data recording time window immediately following a calorimeteric-triggered event and completing the partially recorded off-time collisions in the long integration time window of the MVTX and TPC detectors, one captures additional interactions most efficiently. From an analysis point of view, this is an elegant solution as it avoids any trigger selection bias which would be quite complicated for rare and weak signals such as hadronically decayed heavy-flavor hadrons. The effect of this upgrade can be quantified as shown in Figure D.2, where a 50% increase in the data volume column allows for recording 10% of **all** minimum biased collisions, an increase by two to three orders of magnitude as detailed in Table D.1 (right columns).

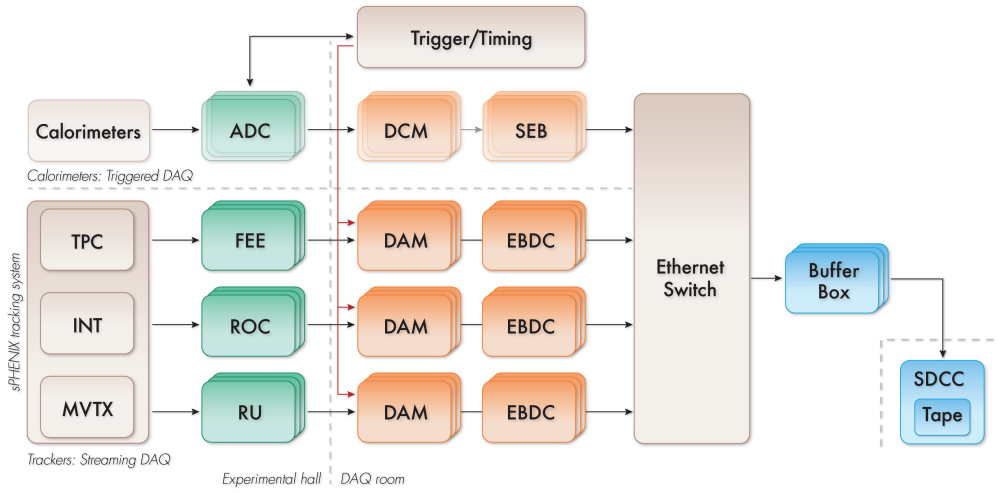

Figure D.1: The hybrid DAQ structure of the sPHENIX tracking detectors, in which all three detectors are read out in a streaming mode. The output of the tracker data streams are throttled appropriately to be in synchrony with calorimeter triggers. Additional tracker data can also be streamed, providing an opportunity to record minimum bias collisions beyond those coming from calorimeter-triggered events.

D.1.1 Hybrid Trigger-Streaming Readout in 2024

In the 2024 run, we plan to implement the first streaming readout DAQ for the tracking detectors to record 10% of the delivered luminosity in addition to the calorimeteric-triggered events. The data rate and data volume is dominated by the time projection chamber which is studied in Figure D.2. With the introduction of the beam crossing angle, the expected data rate with the 10% streaming readout would be much lower than the design specifications and the previous data volume estimates with zero crossing angle assumed in the 2019 sPHENIX computing plan [42].

		Year-2024, triggered DAQ per-1kHz M.B. trigger	Year-2024, w/ str. tracker	Year 2026 w/ str. tracker
M.B. p+p	Data Mode	Each 1k Hz M.B. trigger w/ 4×10^{-4} of M.B. coll. triggered	10% M.B. events str. recorded	100% M.B. events str. recorded
	Stats	1 Billion M.B. evts 0.026 pb^{-1} recorded	250 Billion M.B. evts 6.2 pb^{-1} recorded	3.2 Trillion M.B. evts 80 pb^{-1} recorded
Physics Reach	B $\rightarrow$ D^0 $\rightarrow \pi$K R_{AA} ref.	620 evts	150k evts	2M evts
	D^0 $\rightarrow \pi$K pair Diffusion of c+$\bar{c}$	620 evts	150k evts	2M evts
	$\Lambda_c \rightarrow \pi$K$p$ Charm hadronization	1.3k evts	310k evts	4M evts
	Prompt D^0 $\rightarrow \pi$K Tri-Gluon Corr. via TSSA	0.2M evts	50M evts	0.6B evts

Table D.1: Statistical reach for HF p+p events by channel in different data taking periods and modes, including streaming readout of the tracker.

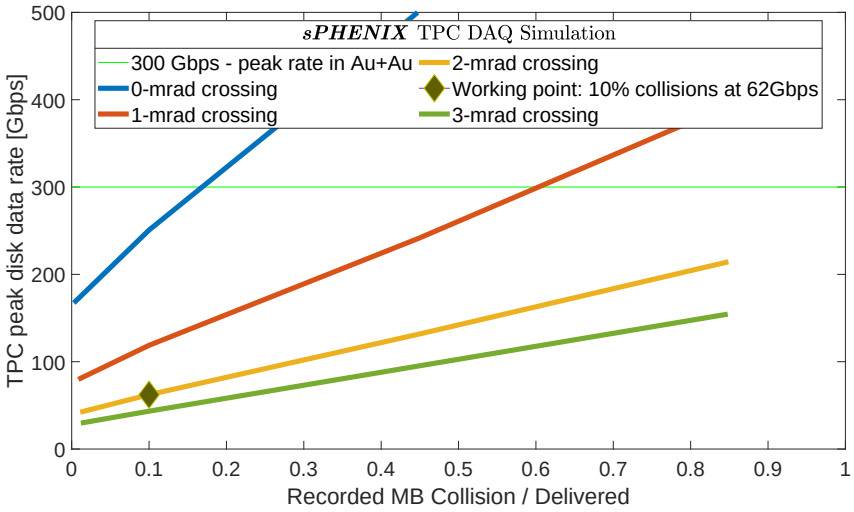

Figure D.2: Choice of operation point between the peak TPC data logging rate and the fraction of M.B. p+p collision recorded. The green horizontal line denotes the peak data logging rate for Au+Au collisions. At similar logging rate and without the beam crossing angle, a minimum of 10–20% of p+p M.B. collisions can be streamed to the raw data file as denoted by the solid blue curve. In the case that a beam cross angle is introduced (red, orange and green curves) the overall data rate can be significantly reduced. The default work point in the 2024 run is with 2 mrad beam crossing angle and record 10% of collisions at 62 Gbps data rate as denoted by the diamond point.

The reason is simply because with the 2 milliradian crossing angle there are far fewer collisions outside of $|z| < 10$ cm that would have still caused hits in the TPC that would have been recorded.

The physics gain is significant, that includes the p+p reference data for the D^0 R_{AA} and the Λ_c/D^0 ratio both of which are critical for the systematic control in understanding the Au+Au data as discussed in Section 3.3. In addition, since the p+p beam is transversely polarized, the single spin asymmetry in the D^0 channel can be measured to gain access of tri-gluon correlation [29, 43], which is further discussed in Section 3.4. All aforementioned physics gains would be first measurements at RHIC and uniquely enabled by the streaming DAQ of the sPHENIX trackers.

D.1.2 Full streaming Readout for Potential 2026–2027 Running

If RHIC runs in 2026 and/or 2027 become available, we would augment the initial DAQ to be able to stream *all* of the data from the sPHENIX tracking detectors for *all* collision species. The curves in Figure D.2 show that as the fraction of streaming data is increase, the TPC data rate increases, and a fully streamed DAQ would have imply a data rate wsignificantly higher than the 2024 working point, shown as a black diamond in the figure. However, assuming even a small beam crossing angle, this data rate would still be below the 300 Gbps bandwidth limit of the full readout system neotiated with the RHIC computing facility. At the expense of a somewhat higher data volume, a full streaming readout of the trackers allows another order of magnitude improvement in the recorded p+p and p+A statistics, whose impact is further quantified in Chapter E.

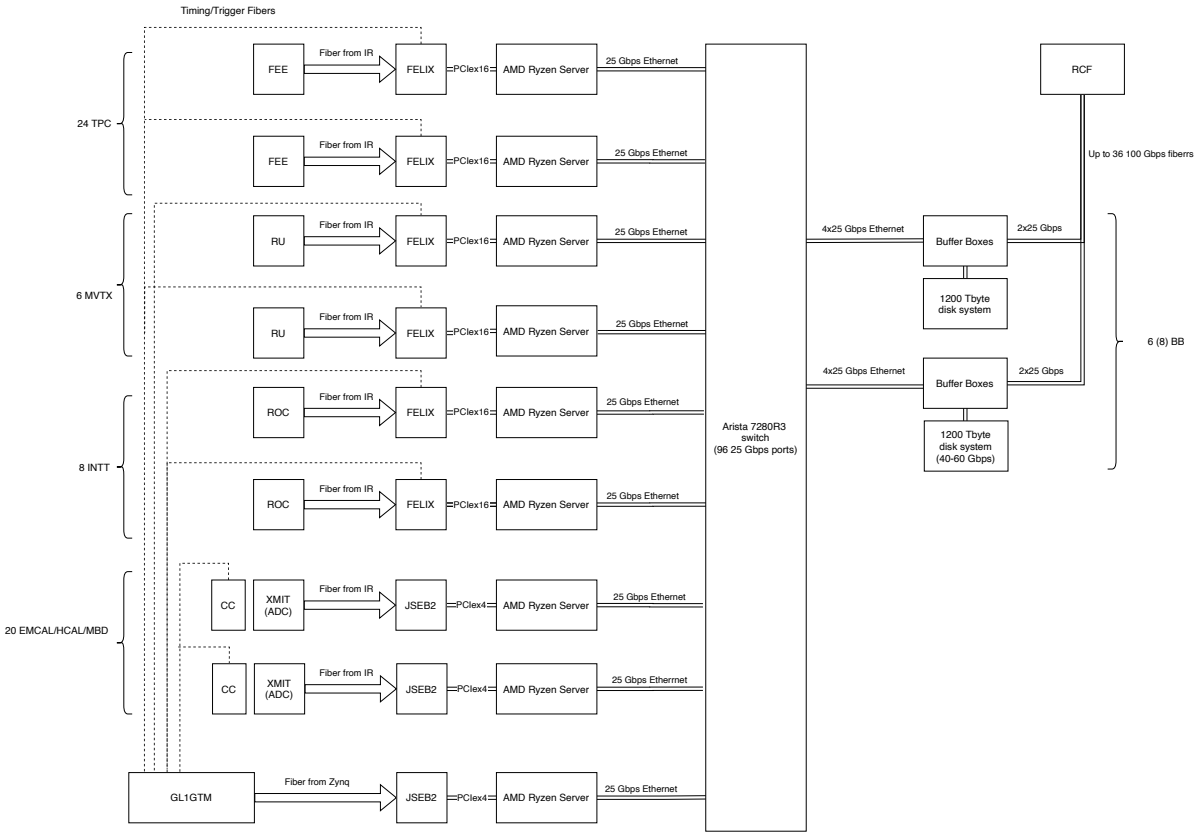

Figure D.3: Block diagram of sPHENIX data acquisition system, showing interfaces to MVTX, INTT, and TPC front end electronics using the ATLAS FELIX interface, and electromagnetic and hadronic calorimeters and Minimum Bias Detector using the DCM2 and JSEB card.

D.1.3 Data Preservation and Data Mining

This upgrade will accumulate a large amount (10–100% of delivered luminosity) of minimum bias polarized $p+p$ data without a trigger bias and with the full sPHENIX tracking capability. Asr RHIC completes its scientific mission at the end of the sPHENIX program, this unique data set would allow future data mining for novel quantum effects such as quantum coherence in particle production. Such future analyses would have the full freedom to define an "event" in the offline software "trigger" that is based on high level objects such as tracklets and final detector alignment and calibrations. These $p+p$ data may be critical for fully understanding the future $e-$Acollision data at the Electron Ion Collider [44].

D.2 De-Multiplexing the Calorimeter Readout

The sPHENIX data acquisition system is designed to acquire events from the front end electronics at 15 kHz with a livetime of 90% or greater. Custom digitizers on the detector have been designed to transmit data over fiber optic cables to computers in the sPHENIX Rack Room which record data to local fileservers before copying the data to the RACF for archiving and analysis. A block

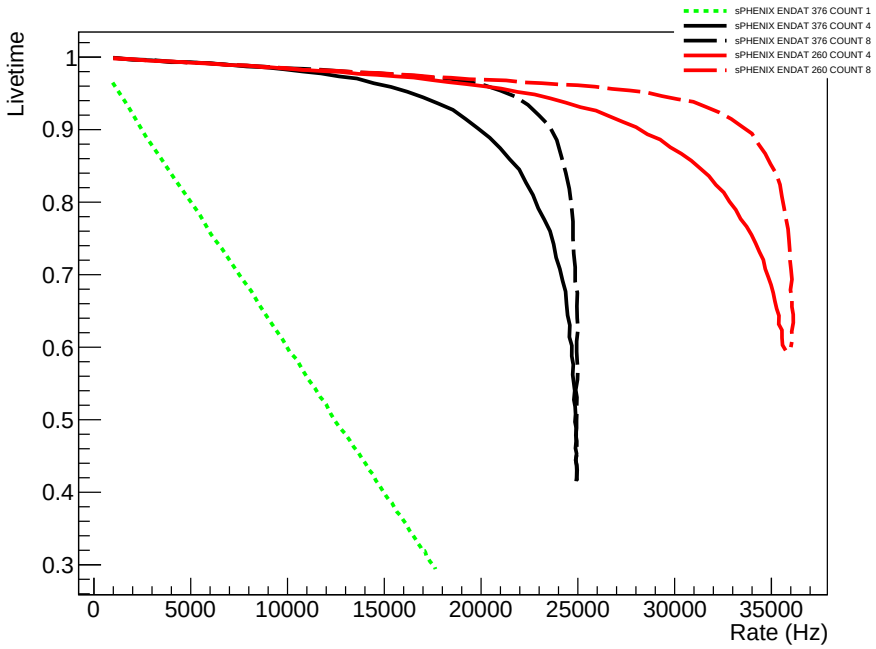

Figure D.4: Livetime as a function of trigger rate for calorimeter digitizers for 1, 4, and 8 event buffering in the front end in the baseline design (black), and with possible future upgrades (red). For comparison, the green line shows the effect of single event buffering, or stop-and-read.

diagram of the system is shown in Figure D.3. The system is designed with high speed links and buffering at several points to achieve the design livetime at a 15 kHz event rate. In the absence of data flow bottlenecks, the livetime is limited by the ADC system used to read out the three calorimeters (EMCal, iHCal and oHCal) and the Minimum Bias Detector.

The ADC system used by the calorimeters uses 60 MHz waveform digitizers to record a fixed number of samples at the time of a Level-1 trigger, which are buffered locally on the detector for 4, and possibly as many as 8, events before serialization and transmission over optical fiber from a digitizer "XMIT" board to second generation Data Collection Modules (DCM II) — reused from the PHENIX experiment — which zero suppress and re-format the data. The sPHENIX baseline design collects data from three ADC modules (192 channels) to one fiber (by way of the XMIT board), and the time to transmit an event ultimately determines the livetime as a function of event rate. Assuming there are no data transmission bottlenecks downstream which would require throttling the data flow, the transmission time for a single event is designed to be about 40 μsec. Buffering events at the digitizer makes it possible to achieve a livetime greater than 90% with 15 kHz of input triggers, but the livetime decreases as the trigger rate approaches 25 kHz, as shown by the black curves in Figure D.4.

A possible upgrade to the ADC system which could nearly double the rate of recorded events while maintaining the 90% livetime would be to decrease the number ADC modules serialized on one fiber in the electromagnetic calorimeter. Reducing the number of ADC boards per fiber to two would not require more crates on the detector, and would decrease the transmission time to about 28 μsec. The pronounced effect of this *de-multiplexing* is shown by the red curves in Figure D.4.

This upgrade would require 64 additional XMIT boards and eight additional DCM II boards as well as some additional electronics, fibers, and crates to serve them. A rough estimate of the cost is $100–150k in electronics and a similar cost for engineering, for a total cost of about $300k. Due to parts obsolescence and continuing advances in electronics, it might be preferable to design a replacement for the DCM II modules, but it is not practical to consider such a project until the baseline electronics is installed and operating.

Appendix E

Potential Beam Use Proposal 2026–2027

Note: The quantitative details in this appendix have not been updated to reflect the latest available C-AD guidance for p+p, p+Au, and Au+Au running since 2022, and no new guidance from C-AD on light ion running has been requested. It is included here for archival reasons to give an illustration of the physics possibilities for continued RHIC running to increase the luminosity for the core collision systems as well as expand the program to include intermediate and light ion collisions.

In this appendix we provide details on a potential additional two years of running in 2026–2027 that presents a further return on investment in sPHENIX and also the entire RHIC program. A possible running plan in these two years was originally requested by ALD Berndt Mueller in previous Beam Use Proposals, which we therefore reproduce here. We highlight that if such a window of opportunity arises this would represent the last opportunity for data taking in heavy-ion mode in this energy regime in our lifetime.

E.1 Proposal Summary

The sPHENIX proposal for such a potential window of opportunity is summarized in Table E.1. The two years assume 28 cryo-weeks in each and with a sPHENIX uptime of 80% with detector operations having reached a mature state. The projected luminosities are documented for the years 2026 and 2027 using guidance from C-AD. For completeness, we detail in the cryo-weeks for the potential 2026 and 2027 runs at the end of this Chapter in Section E.4.

We highlight that key upgrades at very modest cost can have a major increase in the physics impact of these additional years of running. Demultiplexing the calorimeter readout increases the Level-1 trigger accept rate to 30 kHz, doubling the rate of calorimeter data events. Increasing the tracking detectors streaming readout to 100% results in an order of magnitude more data than in the 2024–2025 data-taking period. These upgrade options are detailed in Chapter D.

Table E.1: The recorded luminosity (Rec. Lum.) and sampled luminosity (Samp. Lum.) values are for collisions with z-vertex $|z| < 10$ cm.

Year	Species	$\sqrt{s_{NN}}$ [GeV]	Cryo Weeks	Physics Weeks	Rec. Lum. $\|z\|$ <10 cm	Samp. Lum. $\|z\|$ <10 cm
2026	$p^{\uparrow}p^{\uparrow}$	200	28	15.5	1.0 pb^{-1} [10 kHz] 80 pb^{-1} [100%-*str*]	80 pb^{-1}
–	O+O	200	–	2	18 nb^{-1} 37 nb^{-1} [100%-*str*]	37 nb^{-1}
–	Ar+Ar	200	–	2	6 nb^{-1} 12 nb^{-1} [100%-*str*]	12 nb^{-1}
2027	Au+Au	200	28	24.5	30 nb^{-1} [100%-*str*/DeMux]	30 nb^{-1}

E.2 Au+Au and p+p Physics Reach

First, we start with the Au+Au increased physics reach. In Table E.2 we compare directly the Au+Au recorded and sampled luminosities from the three runs in 2023, 2025, and the potential opportunity in 2027. The upgrades enable a doubling of the Au+Au data set to 30 nb^{-1} or equivalently 200 billion Au+Au events. These events will serve as a permanent archive of Au+Au data, to be mined for any future analysis once RHIC is no longer running heavy ions. There are no trigger biases or selections that would preclude any analysis within the acceptance and performance parameters of sPHENIX.

The impact on the polarized p+p data set is even more substantial, not only for the heavy ion program but also for studies of spin-dependent QCD. The comparison of running p+p in 2024 and 2026 is shown in Table E.3. The striking gain is in the 80 pb^{-1} recorded with the tracking detectors via 100%-*str* mode, more than a factor of ten over the previous data set. There are many measurements, particularly in the heavy-flavor and transverse spin (cold QCD) arena where selective physics triggers are not available and thus the p+p measurements are the statistically limiting factor in the Au+Au-to-p+p comparisons. This enormous data set, with an additional 130 pb^{-1} of data samples for both calorimetric jet and tracking-based measurements, represents an immediate opportunity to advance our precision physics knowledge and to create a permanent archive of data from RHIC.

The substantial increase in statistics translates into ultra-precise measurements of basic observables and the enabling of highly differential observables. Here we show a subset of example projection plots. Figure E.1 (left) shows the improvement in statistical precision for direct photon, jet, and

Table E.2: Summary of Au+Au at 200 GeV running in the sPHENIX Beam Use Proposal. The recorded luminosity (Rec. Lum.) and first sampled luminosity (Samp. Lum.) values are for collisions with z-vertex $|z| < 10$ cm.

Year	Species	$\sqrt{s_{NN}}$ [GeV]	Cryo Weeks	Physics Weeks	Rec. Lum. $\lvert z\rvert$ <10 cm	Samp. Lum. $\lvert z\rvert$ <10 cm
2023	Au+Au	200	24 (28)	9 (13)	3.7 (5.7) nb^{-1}	4.5 (6.9) nb^{-1}
2025	Au+Au	200	24 (28)	20.5 (24.5)	13 (15) nb^{-1}	21 (25) nb^{-1}
2027	Au+Au	200	28	24.5	30 nb^{-1} [100%-*str*/DeMux]	30 nb^{-1}

Table E.3: Summary of p+p at 200 GeV running in the sPHENIX Beam Use Proposal. The recorded luminosity (Rec. Lum.) and sampled luminosity (Samp. Lum.) values are for collisions with z-vertex $|z| < 10$ cm.

Year	Species	$\sqrt{s_{NN}}$ [GeV]	Cryo Weeks	Physics Weeks	Rec. Lum. $\lvert z\rvert$ <10 cm	Samp. Lum. $\lvert z\rvert$ <10 cm
2024	$p^{\uparrow}p^{\uparrow}$	200	24 (28)	12 (16)	0.3 (0.4) pb^{-1} [5 kHz] 4.5 (6.2) pb^{-1} [10%-*str*]	45 (62) pb^{-1}
2026	$p^{\uparrow}p^{\uparrow}$	200	28	15.5	1.0 pb^{-1} [10 kHz] 80 pb^{-1} [100%-*str*]	80 pb^{-1}

charged hadron nuclear modification factor R_{AA} as a function of p_T in 0–10% central Au+Au collisions. The higher luminosity, particularly at high-p_T where underlying event backgrounds are low, will enable a precision decomposition of these jet events. Figure E.1 (right) shows the statistical precision for the "golden-channel" photon + jet distribution. The precision is sufficient that one can then further dissect these events and look for medium response opposite the photon in selections of $x_{J\gamma}$. Another example of a statistically-driven measurement is the azimuthal anisotropy of high p_T probes. Figure E.2 shows the statistical uncertainties for jets with $p_T > 40$ GeV as a function of angle relative to the second-order reaction plane. The precision measurements with Year 4–5 (2026–2027) data included will enable a key constraint on jet quenching calculations embedded in a realistic hydrodynamic expanding background.

The Upsilon measurement is another case where additional precision will enable more differential observations. Figure E.3 (left) shows the increased statistical accuracy for the centrality dependence with the added Year 4-5 (2026-2027) data. Figure E.3 (right) shows the improvement in precision

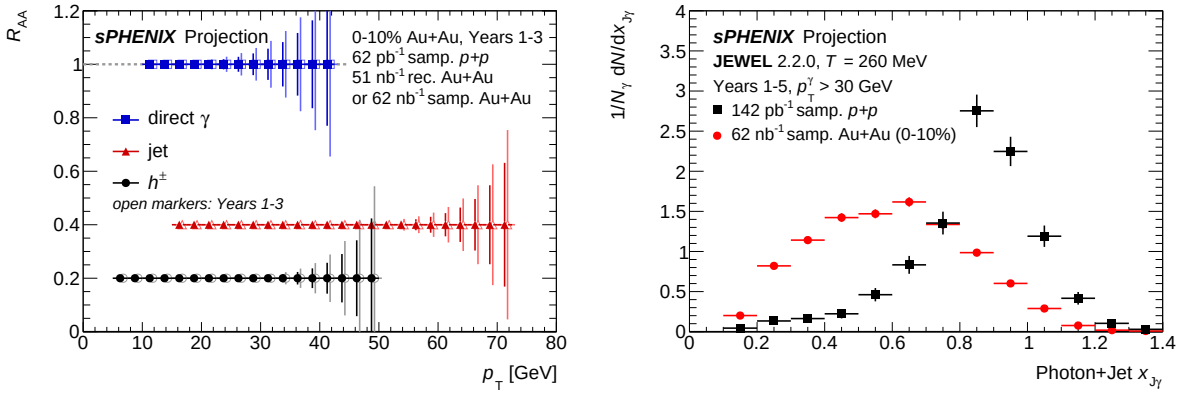

Figure E.1: (left) Nuclear modification factor R_{AA} in 0–10% central Au+Au collisions for direct photons, jets, and charged hadrons as a function of p_T. Shown are the statistical uncertainties from Year 1–3 (2023–2025) running compared with including the additional Year 4–5 (2026–2027) running. (right). Statistical precision for $x_{J\gamma}$ in photon + jet events from additional Year 4–5 (2026–2027) running.

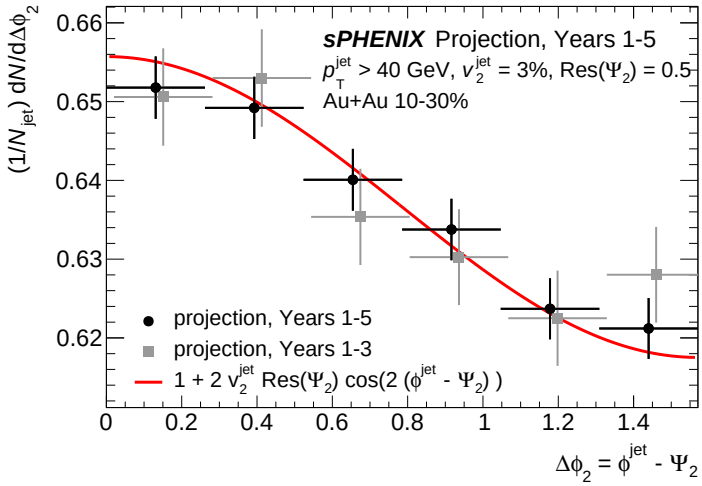

Figure E.2: Statistical projections for the jet yield as a function of the azimuthal distance from the event plane in 10–30% Au+Au events.

for the transverse momentum dependence in the 0–10% most central collisions. Examples of measurements for which the higher luminosity would be valuable are the rapidity dependence for the $\Upsilon(1S)$ and $\Upsilon(2S)$, and correlations measurements, such as azimuthal anisotropies.

The statistical gain from the 2026–2027 data would be beneficial for rare heavy-flavor observables, in particular for exclusive decay channels, HF flow and asymmetries. As shown in Figure E.4, a clean separation of the v_1 for D^0 and $\bar{D}^0$ is expected summing five years of Au+Au data, which would provide quantitative access to the initial magnetic field in heavy-ion collisions [45]. With 100% streaming data acquisition, the D^0 statistics and the uncertainty for the D^0 spin asymmetry A_N are dramatically improved in the polarized p+p collisions as shown in Figure E.5, which provides a strong constraint on the amplitude and p_T dependence of tri-gluon correlations in the

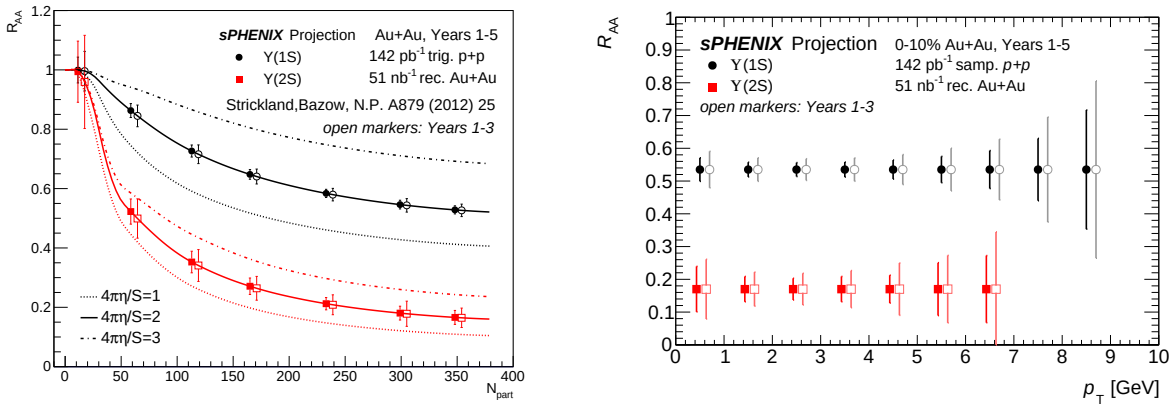

Figure E.3: sPHENIX projected statistical uncertainties, including from background subtraction contributions, for the Upsilon nuclear modification factors as a function of centrality (left) and p_T (right) in the proposed three-year (2023–2025) run plan and then compared with the improved precision adding projected data from 2026–2027.

proton. The collaboration is also studying the viability of full reconstruction of exclusive decay channels such as B_s meson that would provide new information on the strange enhancement and hadronization with the tagging of heavy bottom quark.

Finally, the size of the recorded Au+Au dataset along with the broad capabilities of sPHENIX will allow the community to continue to produce a variety of imaginative and expansive measurements in the years after RHIC has completed data-taking. These include new measurements of correlations and fluctuations, the chiral magnetic effect, the production of soft photons via conversion methods, and others not yet envisioned.

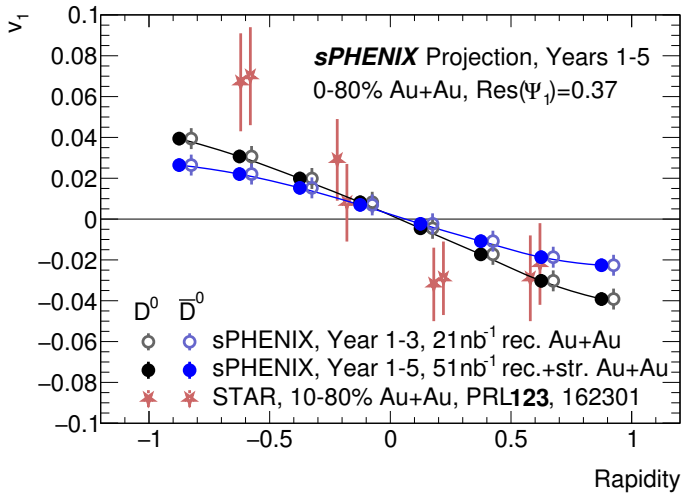

Figure E.4: Projection for direct flow of D^0 and $\bar{D}^0$ mesons (black and blue data points), which is compared with recent results from STAR [46] (red points) and calculations combining effects from the tilted geometry [47] and the initial EM fields [45] (curves).

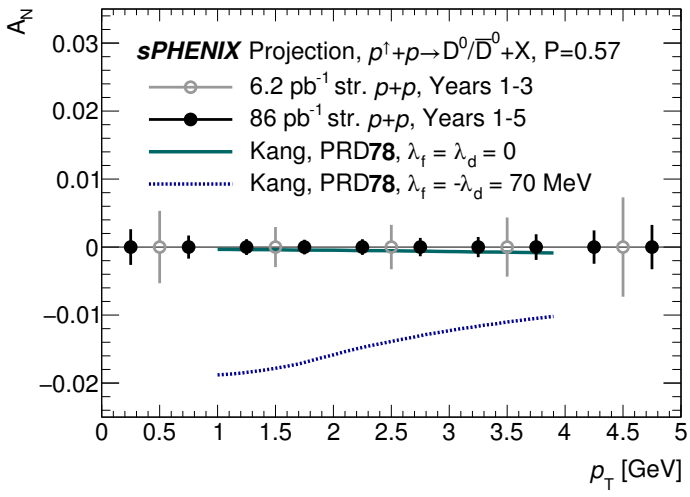

Figure E.5: Statistical projections of transverse spin asymmetry for the D^0 mesons for five years data taking, a dramatic improvement over the initial three-year data discussed in Section 3.4.

E.3 O+O and Ar+Ar Physics Reach

The RHIC program has a 100% track record of learning new physics and gaining insights from every novel nuclear species combinations put into collision. It is a testament to the facility and the constant improvements, including the EBIS source, that have been the lifeblood of the machine. An opportunity to run smaller symmetric collision species, such as O+O and Ar+Ar, is essentially guaranteed to provide key insights and resolve some key outstanding puzzles in the field. Here we outline one possible plan for small systems running. However, the particular running plan in 2026 could ultimately involve different combinations of small nuclei, depending on the discoveries made using 2023–2025 sPHENIX data, those made during the concurrent LHC Run 3 which will potentially include O+O collisions, and developments in theory during that time.

A major open question in the field and an associated major puzzle relates to jet quenching or the lack thereof in small systems, for example p+Au at RHIC and p+Pb at the LHC. Despite a wealth of evidence for collectivity [34], described by hydrodynamics in these small systems, the p_T distribution of charged hadrons, reconstructed jets, and open heavy-flavor hadrons appears nearly unmodified, i.e. $R_{pA} = 1$ within uncertainties. Is there a minimum medium size or lifetime requires for jet quenching phenomena? Does such a minimum value relate to hard struck quarks and gluons having a formation time before scattering in medium or having coherence effects? These are fundamental questions that are needed to fully understand the physics of small systems and to bridge the divide between small and large systems.

The associated major puzzle is that at the LHC in p+Pb collisions there is a definite azimuthal anisotropy for charged hadrons up to $p_T \approx 50$ GeV [41], and D mesons and their decay leptons are observed to have an azimuthal anisotropy as well in p+A and even p+p collisions. In A+A collisions, the high-p_T v_2 is interpreted as differential jet quenching, which would seem impossible in small systems if there is no indication of jet quenching in the nuclear modification factor.

sPHENIX will extend these measurements as part of the p+Au running in 2024 as discussed in Section 3.4.

In principle one can use peripheral Au+Au or Pb+Pb collisions to map out these observables and bridge the divide between large and small systems. However, there are substantial event selection biases that have recently been shown to have caused $R_{AA} < 1$ in peripheral A+A collisions at RHIC and the LHC [48]. Correcting for these biases is challenging particularly if one is teasing out modest modifications in the p_T distribution of order 10–20%. One solution to this problem is to run smaller symmetric nuclear collision species. One can use minimum bias events where there is no event selection bias, and one can also use selected high-multiplicity events where the bias is in the opposite direction to that in Au+Au and thus one can test whether one can correct out this bias.

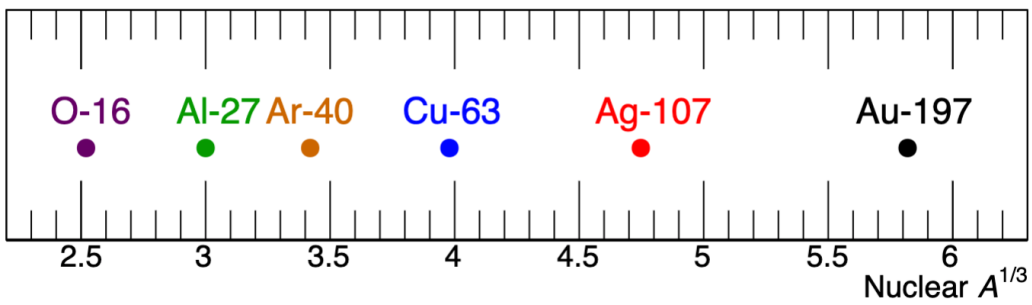

Figure E.6: Various nuclei plotted as a function of $A^{1/3}$.

What is the optimum nuclear collisions species and for how many weeks should one run to collect the necessary data set? Figure E.6 shows the nuclear thickness as it scales with $A^{1/3}$ for different potential nuclei. Monte Carlo Glauber and direct photon NLO rates are combined with C-AD luminosity projections to plot the number of jets and direct photons that can be measured by sPHENIX per week of running as a function of the number of binary collisions N_{coll}, as shown in Figure E.7.

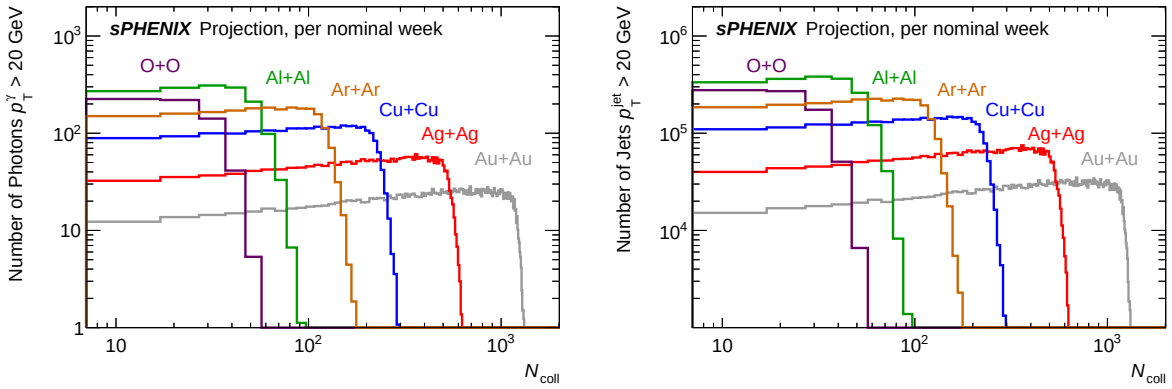

Figure E.7: Number of direct photons (left) and jets (right) with $p_T > 20$ GeV measurable by sPHENIX per nominal week of delivered luminosity as a function of the number of binary collisions.

An optimum balance of system size and running time is closely matched by running two weeks of physics data taking for O+O and Ar+Ar. Using projections from C-AD, even during this short

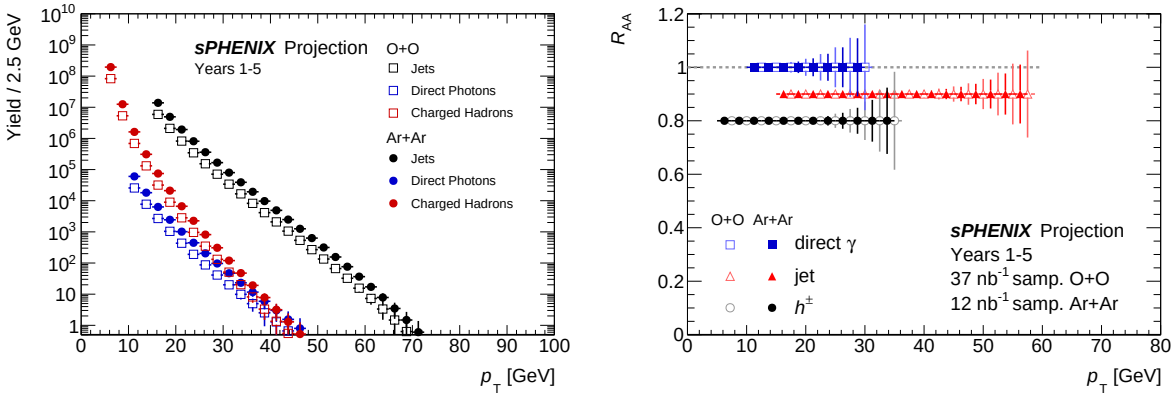

Figure E.8: Projected total yields (left) and R_{AA} (right) for jets, photons, and charged hadrons in O+O and Ar+Ar events taken during a potential sPHENIX run in 2026.

running period, one can measure direct photons beyond 25 GeV and jets out beyond 50 GeV as shown in Figure E.8. The direct photon measurement in particular enables confirmation of minimum bias A-scaling of the cross section as well as any corrections to bias factors in multiplicity-selected events.

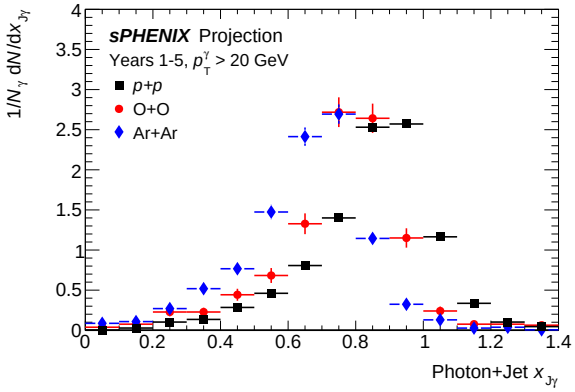

Figure E.9: Projected jet-to-photon p_{T} balance distributions for $p_{\mathrm{T}}^{\gamma} > 20$ GeV in p+p, O+O, and Ar+Ar events taken during a potential sPHENIX run in 2026.

This sample will also enable differential measurements of many quantities. For example, Figure E.9 shows projected x_{Jfl} distributions for $p_{\mathrm{T}}^{\gamma} > 20$ GeV, for which there will be 800 and 1 900 events in O+O and Ar+Ar data, respectively. The projection shows that there will be sufficient data to make a compelling measurement of γ-tagged energy loss in these small symmetric systems. As a note, the projection includes very low values of $x_{\mathrm{J}\gamma} < 0.4$ at which jet measurements may not be feasible. However, the physics effect is primarily at high $x_{\mathrm{J}\gamma}$ since the magnitude of energy loss is expected to be small, and one could use photon–hadron correlations to explore the very low-p_{T} physics.

Figure E.10 (left) shows a projection for the v_2 for charged hadrons as a function of p_{T} for both O+O and Ar+Ar. sPHENIX will have sufficient reach to measure out to $p_{\mathrm{T}} \sim 25$ GeV. In large A+A systems, a non-zero v_2 in this kinematic region, which is far outside the low-p_{T} region governed by hydrodynamic expansion, is conventionally understood to arise from a path-length dependent jet

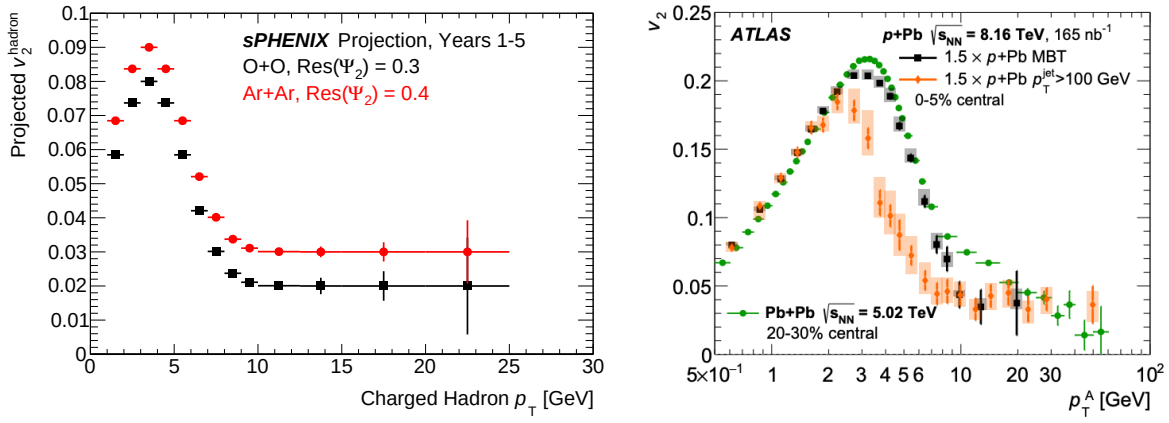

Figure E.10: (Left) Statistical projection for charged hadron v_2 in O+O and Ar+Ar data as a function of p_{T}. (Right) ATLAS high-p_T v_2 in p+Pb and Pb+Pb collisions at the LHC. [41]

energy loss. However, recent results at the LHC, shown in Figure E.10 (right), show that a small, non-zero v_2 is observed even in p+Pb collisions out to 50 GeV, despite no significant energy loss observed in other measurements. Since sPHENIX will be able to make simultaneous measurements of the v_2 and the R_{AA} with high precision in both O+O and Ar+Ar, we can map out the physics of systems with sizes between the p+A and A+A in detail.

Additionally, the related puzzle of heavy-flavor anisotropies in p+p and p+A but with $\mathrm{R}_{pA} \approx 1$ can be tested in these small systems. As shown in Figure E.11, a large minimum bias sample for prompt D^0 can be detected allowing simultaneously high precision measurement of its nuclear modification and v_2. Similar observables can be further extends to other heavy-flavor channels, such as the non-prompt D^0 mesons which provide a window into the heavier of the heavier b-quark in these collision systems. Measurements in O+O and Ar+Ar of heavy-flavor R_{AA} and v_2 are a key part of understanding the physics in these small systems. There are theoretical proposals that the azimuthal anisotropy in small systems for heavy-flavor hadrons and quarkonia comes from initial-state Color Glass Condensate effects. However, this is challenged by the idea that the heavy-flavor particles are correlated with all bulk low-p_T particles that are described by hydrodynamics. These data will provide further tests of any models working towards solving the small system HF puzzle.

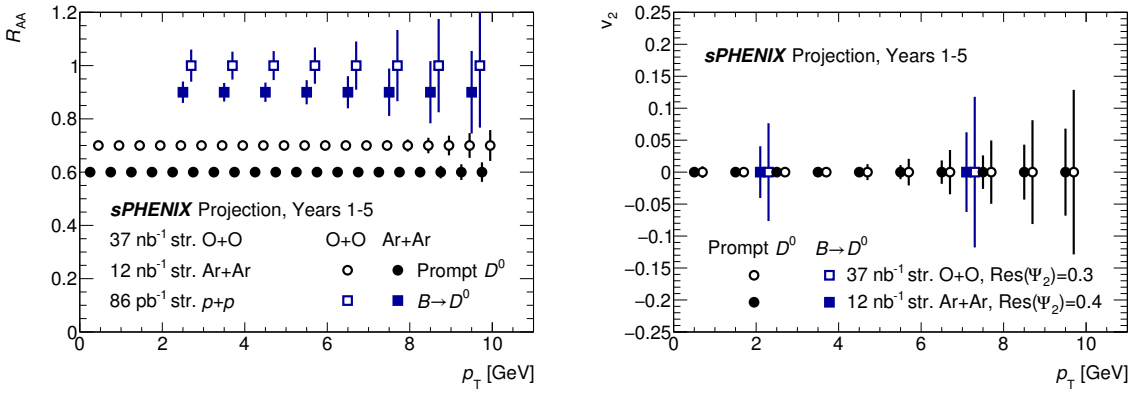

Figure E.11: Projection for R_{AA} (left) and v_2 (right) for prompt (black) and non-prompt (blue) D^0 production in the M.B. O+O (open marker) and Ar+Ar (filled marker) collisions.

E.4 Cryo-Week Details

For completeness, we detail the 28 cryo-weeks of potential running in 2026 and 2027 in Table E.4 and Table E.5 respectively.

Weeks	Designation
0.5	Cool Down from 50 K to 4 K
2.0	Set-up mode 1 ($p^{\uparrow}p^{\uparrow}$ at 200 GeV)
0.5	Ramp-up mode 1 (8 h/night for experiment)
15.5	Data taking mode 1 ($p^{\uparrow}p^{\uparrow}$ Physics)
2.0	Set-up mode 2 (O+O at 200 GeV)
0.5	Ramp-up mode 2 (8 h/night for experiment)
2.0	Data taking mode 2 (O+O Physics)
2.0	Set-up mode 3 (Ar+Ar at 200 GeV)
0.5	Ramp-up mode 3 (8 h/night for experiment)
2.0	Data taking mode 3 (Ar+Ar Physics)
0.5	Controlled refrigeration turn-off
28.0	Total cryo-weeks

Table E.4: Year 2026 run plan for 28 cryo-weeks with $p^{\uparrow}p^{\uparrow}$, O+O, and Ar+Ar 200 GeV collisions.

Weeks	Designation
0.5	Cool Down from 50 K to 4 K
2.0	Set-up mode 1 (Au+Au at 200 GeV)
0.5	Ramp-up mode 1 (8 h/night for experiments)
24.5	Data taking mode 1 (Physics)
0.5	Controlled refrigeration turn-off
28.0	Total cryo-weeks

Table E.5: Year 2027 run plan for 28 cryo-weeks with Au+Au 200 GeV collisions.

Bibliography

[1] Yasuyuki Akiba et al. The Hot QCD White Paper: Exploring the Phases of QCD at RHIC and the LHC. 2 2015. arXiv:1502.02730. 1.1

[2] Ani Aprahamian et al. Reaching for the horizon: The 2015 long range plan for nuclear science. 10 2015. 1.1

[3] M. Arslandok et al. Hot QCD White Paper. 3 2023. arXiv:2303.17254. 1.1

[4] P. Achenbach et al. The Present and Future of QCD. 3 2023. arXiv:2303.02579. 1.1

[5] Ron Belmont et al. Predictions for the sPHENIX physics program. In *RBRC Workshop: Predictions for sPHENIX*, 5 2023. arXiv:2305.15491. 1.1

[6] sPHENIX Technical Design Report. 5 2019. URL: https://indico.bnl.gov/event/7081/. 1.1

[7] sPHENIX preConceptual Design Report. 10 2015. 1.1

[8] A. Adare et al. An Upgrade Proposal from the PHENIX Collaboration. 1 2015. arXiv:1501.06197. 3.1

[9] M. L. Miller, K. Reygers, S. J. Sanders, and P. Steinberg. Glauber modeling in high energy nuclear collisions. *Ann. Rev. Nucl. Part. Sci.*, 57:205–243, 2007. doi:10.1146/annurev.nucl.57.090506.123020. 3.1

[10] Raghav Kunnawalkam Elayavalli and Korinna Christine Zapp. Simulating V+jet processes in heavy ion collisions with JEWEL. *Eur. Phys. J. C*, 76(12):695, 2016. arXiv:1608.03099, doi:10.1140/epjc/s10052-016-4534-6. 3.1

[11] Georges Aad et al. Measurements of azimuthal anisotropies of jet production in Pb+Pb collisions at $\sqrt{s_{NN}} = 5.02$ TeV with the ATLAS detector. 11 2021. arXiv:2111.06606. 3.1

[12] Jaroslav Adam et al. Azimuthal anisotropy of charged jet production in $\sqrt{s_{\mathrm{NN}}}$ = 2.76 TeV Pb-Pb collisions. *Phys. Lett. B*, 753:511–525, 2016. arXiv:1509.07334, doi:10.1016/j.physletb.2015.12.047. 3.1

[13] Albert M Sirunyan et al. First measurement of large area jet transverse momentum spectra in heavy-ion collisions. *JHEP*, 05:284, 2021. arXiv:2102.13080, doi:10.1007/JHEP05(2021)284. 3.1

[14] M. Strickland and D. Bazow. Thermal bottomonium suppression at RHIC and LHC. *Nucl. Phys.*, A879:25–58, 2012. arXiv:1112.2761, doi:10.1016/j.nuclphysa.2012.02.003. 3.5

[15] S. S. Cao, G.Y. Qin, and S. A. Bass. Energy loss, hadronization and hadronic interactions of heavy flavors in relativistic heavy-ion collisions. *Phys. Rev.*, C92:024907, 2015. doi:10.1103/PhysRevC.92.024907. 3.6, 3.7

[16] Min He, Rainer J. Fries, and Ralf Rapp. Heavy-Quark Diffusion and Hadronization in Quark-Gluon Plasma. *Phys. Rev.*, C86:014903, 2012. doi:10.1103/PhysRevC.86.014903. 3.6, 3.7

[17] T. Song, H. Berrehrah, J. M. Torres-Rincon, L. Tolos, D. Cabrera, W. Cassing, and E. Bratkovskaya. Single electrons from heavy-flavor mesons in relativistic heavy-ion collisions. *Phys. Rev.*, C96:014905, 2017. 3.6, 3.7

[18] J.C. Xu, J.F. Liao, and M. Gyulassy. Bridging soft-hard transport properties of quark-gluon plasmas with cujet3.0. *JHEP*, 1602:169, 2016. doi:10.1007/JHEP02(2016)169. 3.6

[19] Jinrui Huang, Zhong-Bo Kang, and Ivan Vitev. Inclusive b-jet production in heavy ion collisions at the LHC. *Phys. Lett.*, B726:251–256, 2013. arXiv:1306.0909, doi:10.1016/j.physletb.2013.08.009. 3.6

[20] Weiyao Ke, Xin-Nian Wang, Wenkai Fan, and Steffen Bass. Study of heavy-flavor jets in a transport approach. 8 2020. arXiv:2008.07622. 3.6

[21] L. Adamczyk et al. Measurement of D^0 Azimuthal Anisotropy at Midrapidity in Au+Au Collisions at $\sqrt{s_{NN}}$=200 GeV. *Phys. Rev. Lett.*, 118(21):212301, 2017. arXiv:1701.06060, doi:10.1103/PhysRevLett.118.212301. 3.7

[22] Guy D. Moore and Derek Teaney. How much do heavy quarks thermalize in a heavy ion collision? *Phys. Rev.*, C71:064904, 2005. arXiv:hep-ph/0412346, doi:10.1103/PhysRevC.71.064904. 3.3

[23] Santosh K. Das, Francesco Scardina, Salvatore Plumari, and Vincenzo Greco. Heavy-flavor in-medium momentum evolution: Langevin versus Boltzmann approach. *Phys. Rev.*, C90:044901, 2014. arXiv:1312.6857, doi:10.1103/PhysRevC.90.044901. 3.3

[24] Zhong-Bo Kang, Jared Reiten, Ivan Vitev, and Boram Yoon. Light and heavy flavor dijet production and dijet mass modification in heavy ion collisions. *Phys. Rev. D*, 99(3):034006, 2019. arXiv:1810.10007, doi:10.1103/PhysRevD.99.034006. 3.8, 3.3

[25] X. Chen et al. sPHENIX simulation Note sPH-HF-2017-002: D^0-meson and B^+-meson production in Au+Au collisions at $\sqrt{s_{NN}} = 200$ GeV for sPHENIX. 2017. URL: http://portal.nersc.gov/project/star/dongx/sPHENIX/sPH-HF-2017-002-v1.pdf. 3.3

[26] sPHENIX simulation Note sPH-HF-2017-001: Heavy Flavor Jet Simulation and Analysis. 2017. URL: https://indico.bnl.gov/event/3959/. 3.3

[27] Hai Tao Li and Ivan Vitev. Inverting the mass hierarchy of jet quenching effects with prompt b-jet substructure. *Phys. Lett. B*, 793:259–264, 2019. arXiv:1801.00008, doi:10.1016/j.physletb.2019.04.052. 3.9, 3.3

[28] Jaroslav Adam et al. First Measurement of Λ_c Baryon Production in Au+Au Collisions at $\sqrt{s_{NN}}$=200 GeV. *Phys. Rev. Lett.*, 124(17):172301, 2020. arXiv:1910.14628, doi:10.1103/PhysRevLett.124.172301. 3.3, 3.10

[29] Zhong-Bo Kang, Jian-Wei Qiu, Werner Vogelsang, and Feng Yuan. Accessing tri-gluon correlations in the nucleon via the single spin asymmetry in open charm production. *Phys. Rev. D*, 78:114013, 2008. arXiv:0810.3333, doi:10.1103/PhysRevD.78.114013. 3.11, D.1.1

[30] Leszek Adamczyk et al. Azimuthal transverse single-spin asymmetries of inclusive jets and charged pions within jets from polarized-proton collisions at $\sqrt{s} = 500$ GeV. *Phys. Rev. D*, 97(3):032004, 2018. arXiv:1708.07080, doi:10.1103/PhysRevD.97.032004. 3.4

[31] L. Adamczyk et al. Transverse spin-dependent azimuthal correlations of charged pion pairs measured in $p^{\uparrow}$+p collisions at $\sqrt{s}$ = 500 GeV. *Phys. Lett. B*, 780:332–339, 2018. arXiv:1710.10215, doi:10.1016/j.physletb.2018.02.069. 3.4

[32] C. Aidala et al. Nuclear Dependence of the Transverse Single-Spin Asymmetry in the Production of Charged Hadrons at Forward Rapidity in Polarized $p + p$, p+Al, and p+Au Collisions at $\sqrt{s_{NN}} = 200$ GeV. *Phys. Rev. Lett.*, 123(12):122001, 2019. arXiv:1903.07422, doi:10.1103/PhysRevLett.123.122001. B.1

[33] Jaroslav Adam et al. Comparison of transverse single-spin asymmetries for forward π^0 production in polarized pp, pAl and pAu collisions at nucleon pair c.m. energy $\sqrt{s_{\rm NN}} = 200$ GeV. *Phys. Rev. D*, 103(7):072005, 2021. arXiv:2012.07146, doi:10.1103/PhysRevD.103.072005. B.1

[34] James L. Nagle and William A. Zajc. Small System Collectivity in Relativistic Hadronic and Nuclear Collisions. *Ann. Rev. Nucl. Part. Sci.*, 68:211–235, 2018. arXiv:1801.03477, doi:10.1146/annurev-nucl-101916-123209. B.3, E.3

[35] C. Aidala et al. Measurements of Multiparticle Correlations in d + Au Collisions at 200, 62.4, 39, and 19.6 GeV and p + Au Collisions at 200 GeV and Implications for Collective Behavior. *Phys. Rev. Lett.*, 120(6):062302, 2018. arXiv:1707.06108, doi:10.1103/PhysRevLett.120.062302. B.3

[36] C. Aidala et al. Creation of quark–gluon plasma droplets with three distinct geometries. *Nature Phys.*, 15(3):214–220, 2019. arXiv:1805.02973, doi:10.1038/s41567-018-0360-0. B.3

[37] U. A. Acharya et al. Kinematic dependence of azimuthal anisotropies in $p + Au$, $d + Au$, and $^3He + Au$ at $\sqrt{s_{NN}} = 200$ GeV. *Phys. Rev. C*, 105(2):024901, 2022. arXiv:2107.06634, doi:10.1103/PhysRevC.105.024901. B.3

[38] A. M. Sirunyan et al. Elliptic flow of charm and strange hadrons in high-multiplicity pPb collisions at $\sqrt{s_{\rm NN}} = 8.16$ TeV. *Phys. Rev. Lett.*, 121(8):082301, 2018. arXiv:1804.09767, doi:10.1103/PhysRevLett.121.082301. B.3, B.4

[39] Jaroslav Adam et al. D-meson production in p-Pb collisions at $\sqrt{s_{\rm NN}}$ =5.02 TeV and in pp collisions at $\sqrt{s}$ =7 TeV. *Phys. Rev. C*, 94(5):054908, 2016. arXiv:1605.07569, doi:10.1103/PhysRevC.94.054908. B.3

[40] Georges Aad et al. Measurement of azimuthal anisotropy of muons from charm and bottom hadrons in pp collisions at $\sqrt{s} = 13$ TeV with the ATLAS detector. *Phys. Rev. Lett.*, 124(8):082301, 2020. arXiv:1909.01650, doi:10.1103/PhysRevLett.124.082301. B.3

[41] Georges Aad et al. Transverse momentum and process dependent azimuthal anisotropies in $\sqrt{s_{\mathrm{NN}}} = 8.16$ TeV p+Pb collisions with the ATLAS detector. *Eur. Phys. J. C*, 80(1):73, 2020. arXiv:1910.13978, doi:10.1140/epjc/s10052-020-7624-4. B.3, E.3, E.10

[42] sPH-COMP-2019-001: sPHENIX computing plan. 2019. URL: https://indico.bnl.gov/event/6659/. D.1.1

[43] Yuji Koike and Shinsuke Yoshida. Probing the three-gluon correlation functions by the single spin asymmetry in $p^{\uparrow}p \to DX$. *Phys. Rev. D*, 84:014026, 2011. arXiv:1104.3943, doi:10.1103/PhysRevD.84.014026. D.1.1

[44] A. Accardi et al. Electron Ion Collider: The Next QCD Frontier - Understanding the glue that binds us all. 2012. arXiv:1212.1701. D.1.3

[45] Gabriele Coci, Lucia Oliva, Salvatore Plumari, Santosh Kumar Das, and Vincenzo Greco. Direct flow of heavy mesons as unique probe of the initial Electro-Magnetic fields in Ultra-Relativistic Heavy Ion collisions. *Nucl. Phys. A*, 982:189–191, 2019. arXiv:1901.05394, doi:10.1016/j.nuclphysa.2018.08.020. E.2, E.4

[46] Jaroslav Adam et al. First Observation of the Directed Flow of D^0 and $\overline{D^0}$ in Au+Au Collisions at $\sqrt{s_{\mathrm{NN}}}$ = 200 GeV. *Phys. Rev. Lett.*, 123(16):162301, 2019. arXiv:1905.02052, doi:10.1103/PhysRevLett.123.162301. E.4

[47] Sandeep Chatterjee and Piotr Bożek. Large directed flow of open charm mesons probes the three dimensional distribution of matter in heavy ion collisions. *Phys. Rev. Lett.*, 120(19):192301, 2018. arXiv:1712.01189, doi:10.1103/PhysRevLett.120.192301. E.4

[48] Constantin Loizides and Andreas Morsch. Absence of jet quenching in peripheral nucleus–nucleus collisions. *Phys. Lett. B*, 773:408–411, 2017. arXiv:1705.08856, doi:10.1016/j.physletb.2017.09.002. E.3